Guanosine tetra- and pentaphosphate increase antibiotic tolerance by reducing reactive oxygen species production in *Vibrio cholerae*

Received for publication, October 11, 2017, and in revised form, February 16, 2018 Published, Papers in Press, February 23, 2018, DOI 10.1074/jbc.RA117.000383

Hwa Young Kim[‡§], **Junhyeok Go**[‡§], **Kang-Mu Lee**[‡§], **Young Taek Oh**[‡¶1], **and Sang Sun Yoon**[‡§2]

From the [‡]*Department of Microbiology and Immunology, Brain Korea 21 PLUS Project for Medical Science, and the* [§]*Institute for Immunology and Immunological Diseases, Yonsei University College of Medicine, Seoul 03722, Korea and the* [¶]*Freshwater Bioresources Utilization Division, Nakdonggang National Institute of Biological Resources, SangJu 37242, Korea*

Edited by F. Peter Guengerich

The pathogen *Vibrio cholerae* is the causative agent of cholera. Emergence of antibiotic-resistant *V. cholerae* strains is increasing, but the underlying mechanisms remain unclear. Herein, we report that the stringent response regulator and stress alarmone guanosine tetra- and pentaphosphate ((p)ppGpp) significantly contributes to antibiotic tolerance in *V. cholerae*. We found that N16961, a pandemic *V. cholerae* strain, and its isogenic (p)ppGpp-overexpressing mutant Δ*relA*Δ*spoT* are both more antibiotic-resistant than (p)ppGpp^0 (Δ*relA*Δ*relV*Δ*spoT*) and Δ*dksA* mutants, which cannot produce or utilize (p)ppGpp, respectively. We also found that additional disruption of the aconitase B–encoding and tricarboxylic acid (TCA) cycle gene *acnB* in the (p)ppGpp^0 mutant increases its antibiotic tolerance. Moreover, expression of TCA cycle genes, including *acnB*, was increased in (p)ppGpp^0, but not in the antibiotic-resistant Δ*relA*Δ*spoT* mutant, suggesting that (p)ppGpp suppresses TCA cycle activity, thereby entailing antibiotic resistance. Importantly, when grown anaerobically or incubated with an iron chelator, the (p)ppGpp^0 mutant became antibiotic-tolerant, suggesting that reactive oxygen species (ROS) are involved in antibiotic-mediated bacterial killing. Consistent with that hypothesis, tetracycline treatment markedly increased ROS production in the antibiotic-susceptible mutants. Interestingly, expression of the Fe(III) ABC transporter substrate–binding protein FbpA was increased 10-fold in (p)ppGpp^0, and *fbpA* gene deletion restored viability of tetracycline-exposed (p)ppGpp^0 cells. Of note, FbpA expression was repressed in the (p)ppGpp-accumulating mutant, resulting in a reduction of intracellular free iron, required for the ROS-generating Fenton reaction. Our results indicate that (p)ppGpp-mediated suppression of central metabolism and iron uptake reduces antibiotic-induced oxidative stress in *V. cholerae*.

This work was supported by National Research Foundation (NRF) of Korea Grants 2017R1A2A2A05019987, 2015M3C9A2054024, 2014R1A1A2056139, 2014R1A4A1008625, and 2017M3A9F3041233, funded by the Korean government. The authors declare that they have no conflicts of interest with the contents of this article.

This article contains Figs. S1–S4.

[1] To whom correspondence may be addressed: Freshwater Bioresources Utilization Division, Nakdonggang National Institute of Biological Resources, SangJu-si 37242, Korea. Tel.: 82-54-530-0932; Fax: 82-54-530-0949; E-mail: ohyt@nnibr.re.kr.

[2] To whom correspondence may be addressed: Dept. of Microbiology and Immunology, Yonsei University College of Medicine, 250 Seongsanno, Seodaemun-gu Seoul 120-752, Korea. Tel.: 82-2-2228-1824; Fax: 82-2-392-7088; E-mail: sangsun_yoon@yuhs.ac.

Cholera, the epidemic acute diarrheal disease caused by *Vibrio cholerae*, occurs in many developing countries that have poor sanitation (1). The toxigenic strains express various pathogenic factors, including toxin-co-regulated pilus and cholera toxin (CT)[3] to acquire the host environmental niche where it survives in the acidic gastric conditions and enters the small intestine (1–5). These virulence factors permit substantial fluid transport from epithelial cells to lumen, which leads to severe watery diarrhea. Thus, treatments mainly used for cholera patients are oral or intravenous hydration therapy that are effective for reducing stool output (6). According to the cholera treatment guidelines from the World Health Organization and the Centers for Disease Control and Prevention, antibiotic treatment in conjunction with an oral rehydration solution (ORS) is recommended for patients who have severe symptoms or are seriously dehydrated and continue to pass a large amount of stool (7). By evaluating many antibiotics, those that are effective at (i) reducing stool output, (ii) reducing the duration of diarrhea, and (iii) inducing bacterial shedding have been selected for treating cholera patients (8–12). Antibiotic treatment in conjunction with ORS allows patients to recover more rapidly compared with ORS treatment alone. Tetracycline is the most effective antibiotic to reduce the cholera morbidity (8). However, doxycycline, a proxy for tetracycline, is currently the first-line drug of choice for cholera treatment due to its easy administration and low dosage requirement compared with tetracycline (13). Alternative drugs for treatment include chloramphenicol, erythromycin, azithromycin, and furazolidone. This provides drug treatment flexibility dependent on infected regions or antibiotic resistance rates. These antibiotics are only administered in combination with rehydration therapy and are not permitted to be used for the prophylaxis of cholera infection to prevent the induction of antibiotic resistance (14, 15). Recently, most isolates of *V. cholerae* O1 serotype from patient stools showed resistance to antibiotics that are commonly used

[3] The abbreviations used are: CT, cholera toxin; (p)ppGpp, guanosine tetra- and pentaphosphate; TCA, tricarboxylic acid; ROS, reactive oxygen species; SR, stringent response; ABC, ATP-binding cassette; ORS, oral rehydration solution; Tc, tetracycline; Em, erythromycin; Cp, chloramphenicol; SHX, serine hydroxamate; LB, Luria–Bertani medium; cfu, colony-forming unit(s); RPKM, reads per kilobase per million mapped; NAC, *N*-acetylcysteine; OH$^\bullet$, hydroxyl radical; Tn, transposon.

for cholera treatment (16–20), but with no clear underlying mechanisms.

In our previous studies, we revealed that stringent response (SR) regulates *V. cholerae* viability and virulence by providing the bacterium with increased fitness in unfavorable environments (21, 22). SR is characterized as one of the global regulatory systems in bacteria, which is activated by a variety of growth-inhibiting stresses (23). SR induces rapid adaptation under various stress conditions via (p)ppGpp accumulation (24). (p)ppGpp, known as a stress alarmone, forms a complex with RNA polymerase and induces profound reprogramming of global gene expression, which leads to growth arrest (25–27). In most Gram-negative bacteria, (p)ppGpp production is regulated by two enzymes, RelA and SpoT (24, 28). RelA, a monofunctional synthetase, recognizes the uncharged tRNA at the A site of a ribosome, and it starts to synthesize (p)ppGpp. SpoT is the bifunctional enzyme that has both synthetase and hydrolase domains but shows mostly strong hydrolysis and weak synthetase activities. In the case of *V. cholerae*, it has an additional novel (p)ppGpp synthetase called RelV, which loses its N-terminal hydrolase domain (29, 30). Because this enteric pathogen encounters the host-derived immune system during infection, human intestinal environments have the potential to influence nutrient availability to and the viability of *V. cholerae* (1, 31).

Interestingly, recent studies have reported that SR-mediated transcriptional switching impacts bacterial physiology and increases antibiotic resistance (32–34). For example, (p)ppGpp accumulation raises penicillin resistance by inhibiting peptidoglycan synthesis in both Gram-positive and -negative bacteria (35–38). This is not limited to β-lactam antibiotics, and the resistance to other antimicrobials is also linked to (p)ppGpp accumulation (39, 40). It has been suggested that SR-mediated growth defects reduce antibiotic sensitivity, but this hypothesis is not fully understood. Recently, some studies have suggested that decreased levels of superoxide dismutase and catalase activities in SR mutants are associated with susceptibility to multiclasses of antibiotics (41, 42). This report described the famous mechanistic model that different bactericidal antibiotics, regardless of their primary drug target, had a common pathway that generated deleterious ROS (43). According to this concept, ROS formation following antibiotic treatment enhances antibiotic lethality as well as the interaction with their traditional targets. Importantly, this ROS stress is derived from alterations of bacterial physiology, including hyperactivation of central metabolism and cellular respiration and disruption of iron homeostasis, by disrupting specific drug targets (43–45). It might seem strange that antibiotic treatment induces the overflow of metabolism, but to support this idea, many reports have described the transcriptomic and proteomic response to the bactericidal antibiotics (43, 44). Therefore, we hypothesized that the potential capacity for reducing oxidative stress is essential for bacteria to survive during antibiotic treatment.

In this study, we showed that (p)ppGpp accumulation induced antibiotic resistance in *V. cholerae* by suppressing its central metabolism. We investigated the molecular basis of the specific physiology in (p)ppGpp-null *V. cholerae* that restored their viability against antibiotics when the *acnB* gene was totally abolished. Additionally, we showed that the (p)ppGpp-nonproducing *V. cholerae* mutant carried a higher level of intracellular free iron, the crucial source of ROS production. This report provides a novel insight into the stepwise regulation of SR that contributes to defend against oxidative stress following antibiotic treatment.

Results

(p)ppGpp-accumulated V. cholerae exhibits antibiotic tolerance

SR regulates bacterial responses to overcome unfavorable growth conditions in *V. cholerae*. To explore whether *V. cholerae* develops antibiotic tolerance in an SR-dependent manner, we measured survival rates of a range of SR-related mutant strains of *V. cholerae*. Front-line drugs for cholera treatment, tetracycline (Tc), erythromycin (Em), and chloramphenicol (Cp), were used for the bacterial treatments. To elucidate whether antibiotic tolerance was specifically induced by (p)ppGpp accumulation, we first chemically induced (p)ppGpp overproduction in N16961, a seventh pandemic O1 *V. cholerae* strain. When N16961 was treated for 2 h with serine hydroxamate (SHX), a serine analogue that activates SR by mimicking amino acid starvation (41), a marked increase in (p)ppGpp production was induced (Fig. 1*A*). Although ppGpp and pppGpp were not clearly distinguished in our TLC assay, SHX-treated N16961 produced dramatically abundant (p)ppGpp compared with untreated controls (Fig. 1*A*). To assess the effect of (p)ppGpp accumulation on bacterial survival under antibiotic stress, we treated N16961 grown in Luria–Bertani medium (LB) or LB + SHX with varying concentrations of Tc, Em, or Cp for 4 h. Loss of viability was detected in LB-grown N16961. Complete killing was observed after 4 h of treatment with 10 μg/ml Tc (Fig. 1*B*), 60 μg/ml Em (Fig. 1*C*), and 25 μg/ml Cp (Fig. 1*D*). SHX-treated bacterial cells, however, were tolerant to the same antibiotic treatment and maintained their viability under conditions lethal to the control groups (Fig. 1, *B–D*). Although the extent to which these changes occurred was similar in all instances, bacterial viability was least affected in the Tc-treated group, with $\sim 10^6$ cfu/ml recovered even after treatment with the 20 μg/ml concentration (Fig. 1*B*). These results suggest that a clear mechanistic link probably exists between SR and antibiotic tolerance in *V. cholerae*.

To further elucidate the effect of intracellular (p)ppGpp accumulation on bacterial susceptibility to antibiotics in *V. cholerae*, we tested isogenic Δ*relA*Δ*spoT* double and Δ*relA*Δ*relV*Δ*spoT* (termed (p)ppGpp^0) triple mutant strains. The Δ*relA*Δ*spoT* mutant showed highly elevated levels of (p)ppGpp production due to (i) the action of RelV, an additional enzyme involved in (p)ppGpp biosynthesis and (ii) the lack of SpoT that hydrolyzes (p)ppGpp (21). The (p)ppGpp^0 mutant, which lacked all enzymes involved in (p)ppGpp metabolism, was found to produce no (p)ppGpp (21). The level of (p)ppGpp produced in the Δ*relA*Δ*spoT* mutant was similar to that in the SHX-treated N16961 cells, whereas no (p)ppGpp was produced in the (p)ppGpp^0 triple mutant (Fig. 1*A*). We also included a Δ*dksA* mutant, defective in DksA, that binds to RNA polymerase to facilitate the function of (p)ppGpp during SR (46). The capability of the Δ*dksA* mutant to produce (p)ppGpp was

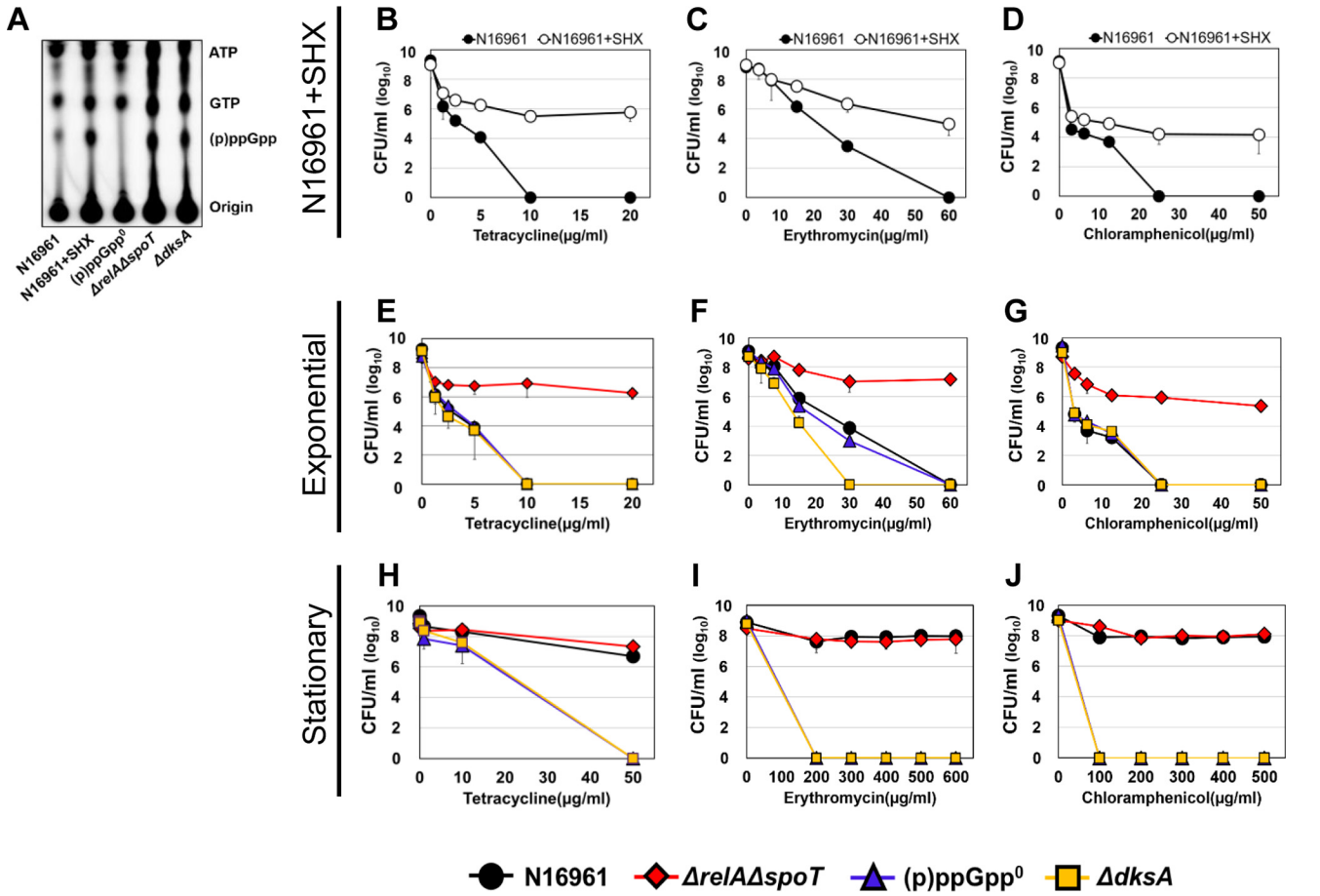

Figure 1. Effects of (p)ppGpp on viability of *V. cholerae* strains against clinically used antibiotics. *A*, detection of (p)ppGpp accumulation pattern in wildtype N16961 by TLC. Wildtype N16961 was divided into two groups and grown in LB supplemented with or without SHX in the presence of [^{32}P]orthophosphate for 2 h. Cellular extracts were prepared and analyzed in TLC. Δ*relA*Δ*spoT*, (p)ppGpp^0, and Δ*dksA* mutants were also grown with [^{32}P]orthophosphate and processed for the TLC assay. *B–J*, bacterial viabilities under various clinically used antibiotics were measured in each growth condition. Wildtype N16961 and various (p)ppGpp-associated mutant strains were inoculated in LB and aerobically grown to each growth stage. Aliquots of each culture were resuspended in several concentrations of antibiotic-containing LB broth, sampled at 4 h post-inoculation, and 10-fold serially diluted to assess the number of cfu.

not affected, as shown in Fig. 1*A*. Because (p)ppGpp levels are known to accumulate as bacterial cells enter the stationary phase (28), we also examined how each bacterial strain, harvested at either the exponential or stationary phase, responded to antibiotic stresses.

When exponential-phase cells were treated with antibiotics, (p)ppGpp^0 and Δ*dksA* mutant strains as well as the WT strain N16961 invariably lost their viability. The Δ*relA*Δ*spoT* mutant, which accumulates intracellular (p)ppGpp, was found to be the only strain that maintained viability (Fig. 1, *E–G*). In contrast, bacterial strains harvested at the stationary phase displayed marked differences from those grown in the exponential phase. Whereas the Δ*relA*Δ*spoT* mutant continued to be antibiotic-tolerant, WT N16961 was also found to be tolerant to the same antibiotic treatment (Fig. 1, *H–J*). Furthermore, these two strains developed tolerance to significantly higher concentrations of antibiotics. Their viabilities were not affected even in the presence of 50 μg/ml Tc, 600 μg/ml Em, or 500 μg/ml Cp, respectively.

To further verify the role of (p)ppGpp in conferring antibiotic tolerance in *V. cholerae*, we tested the antibiotic-susceptible (p)ppGpp^0 mutant harboring pRelV$_{BAD}$, a plasmid that can express the *relV* gene via an arabinose-inducible promoter. When the *relV* gene was expressed, the mutant cells became tolerant to Tc treatment (Fig. S1). Restored tolerance was observed in cells harvested at either growth phase (Fig. S1, *A* and *B*). Such a restoration was not detected in the mutant transformed with a control plasmid. Together, these results demonstrated that the ability to produce and utilize (p)ppGpp, a SR regulator, was critically important in affecting *V. cholerae* susceptibility to antibiotics.

Mutations in the acnB gene resulted in increased tolerance to antibiotic stresses

To provide a mechanistic insight into the increased antibiotic susceptibility of the (p)ppGpp^0 mutant, we sought to identify additional mutations that rendered the mutant tolerant to antibiotic treatments. To achieve this goal, we constructed a transposon (Tn) insertion library of the (p)ppGpp^0 mutant and looked for mutants that survived Tc treatment. Experimental procedures are described in Fig. 2*A*. After three successive subcultures in Tc-containing media, we recovered seven mutants that exhibited unencumbered growth. Subsequent analysis indicated that these mutants harbored Tn insertions in the *acnB* gene encoding a TCA cycle enzyme, aconitase B (Fig. 2*B*). Importantly, Tn insertion was found to occur at different loca-

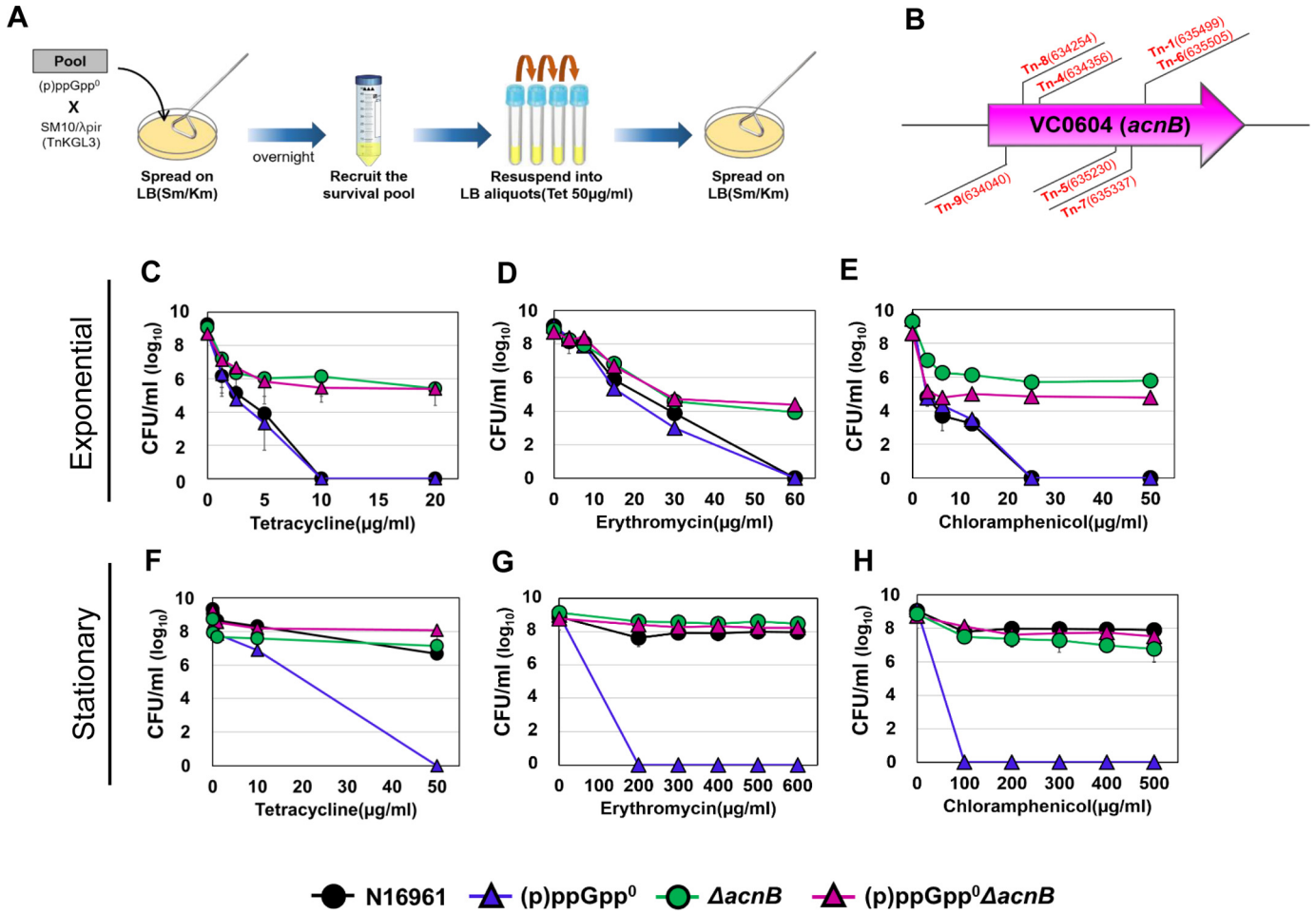

Figure 2. Screening of Tn-insertion mutant strains, derived from the (p)ppGpp^0 strain, which recovered viability under antibiotic treatment. *A*, Tn-insertion mutants, derived from the (p)ppGpp^0 mutant, that survived in the presence of a lethal concentration of tetracycline (50 μg/ml) were selected. Tetracycline was treated three times every 4 h to the entire recruited culture. *B*, a genetic map of the *acnB* gene (VC0604) in *V. cholerae*. *Arrowheads* indicate the positions of Tn insertions. *C–H*, bacterial viability of *acnB*-deletion mutants under tetracycline (*C* and *F*), erythromycin (*D* and *G*), and chloramphenicol (*E* and *H*) treatments. Aliquots of each culture were resuspended in several concentrations of antibiotic-containing LB broth, sampled at 4 h post-inoculation, and serially diluted for cfu counting.

tions of the gene in each of these mutants (Fig. 2*B*), suggesting that independent mutational events resulted in an identical consequence. We then introduced an in-frame deletion of the *acnB* gene into N16961 and (p)ppGpp^0 mutants and measured bacterial responses to the antibiotic treatments. Notably, the viability of bacterial cells, when harvested at the exponential phase, was dramatically increased in both Δ*acnB* and the quadruple (p)ppGpp^{0}Δ*acnB* mutants compared with their parental strains (Fig. 2, *C–E*). cfu of up to ~10^6/ml were observed following Tc (Fig. 2*C*) and Cp (Fig. 2*E*) treatments, whereas ~10^4/ml was recovered after treatment with Em (Fig. 2*D*). Bacterial cells remained viable even in the presence of the highest concentrations of antibiotics. When the (p)ppGpp^{0}Δ*acnB* quadruple mutant, harvested at the stationary phase, was treated with antibiotics, higher levels of bacterial survival were detected (Fig. 2, *F–H*).

Importantly, when the plasmid-born *acnB* gene was expressed by the arabinose-inducible promoter, bacterial strains became susceptible to Tc treatments (Fig. S2). Consistent with previous results, sharper decreases in bacterial viability were detected when using exponential-phase cells (Fig. S2, *A* and *C*). Together, these results demonstrated that deletion of the *acnB* gene conferred a survival advantage to *V. cholerae* in the presence of antibiotic stresses.

Intracellular (p)ppGpp levels inversely regulate TCA cycle activity, which affects bacterial growth and cell morphology

Aconitase B, encoded by *acnB*, is the enzyme that catalyzes the interconversion of citrate and isocitrate in the TCA cycle. To examine whether the bacterial TCA cycle was regulated depending on the intracellular concentration of (p)ppGpp, we monitored transcript levels of genes encoding TCA cycle enzymes by RNA-sequencing analysis. First, *acnB* gene expression was ~3-fold higher in the (p)ppGpp^0 mutant than in the N16961 or in the (p)ppGpp-accumulating Δ*relA*Δ*spoT* mutant (Fig. 3*A*). It is of note that N16961 also possesses the *acnA* gene, which encodes a phylogenetically distinct aconitase. However, its expression was not detected in all three strains, indicating that aconitase B is probably the major enzyme in the TCA cycle (Fig. 3*A*). Expressions of *mdh*, *gltA*, *icd*, *sucA*, *sucC*, and *sucD* genes were also noticeably increased in the (p)ppGpp^0 mutant, whereas their expressions were decreased (albeit to varying degrees) in the Δ*relA*Δ*spoT* mutant (Fig. 3*A*). Although clear (p)ppGpp dependences were not observed in transcriptional

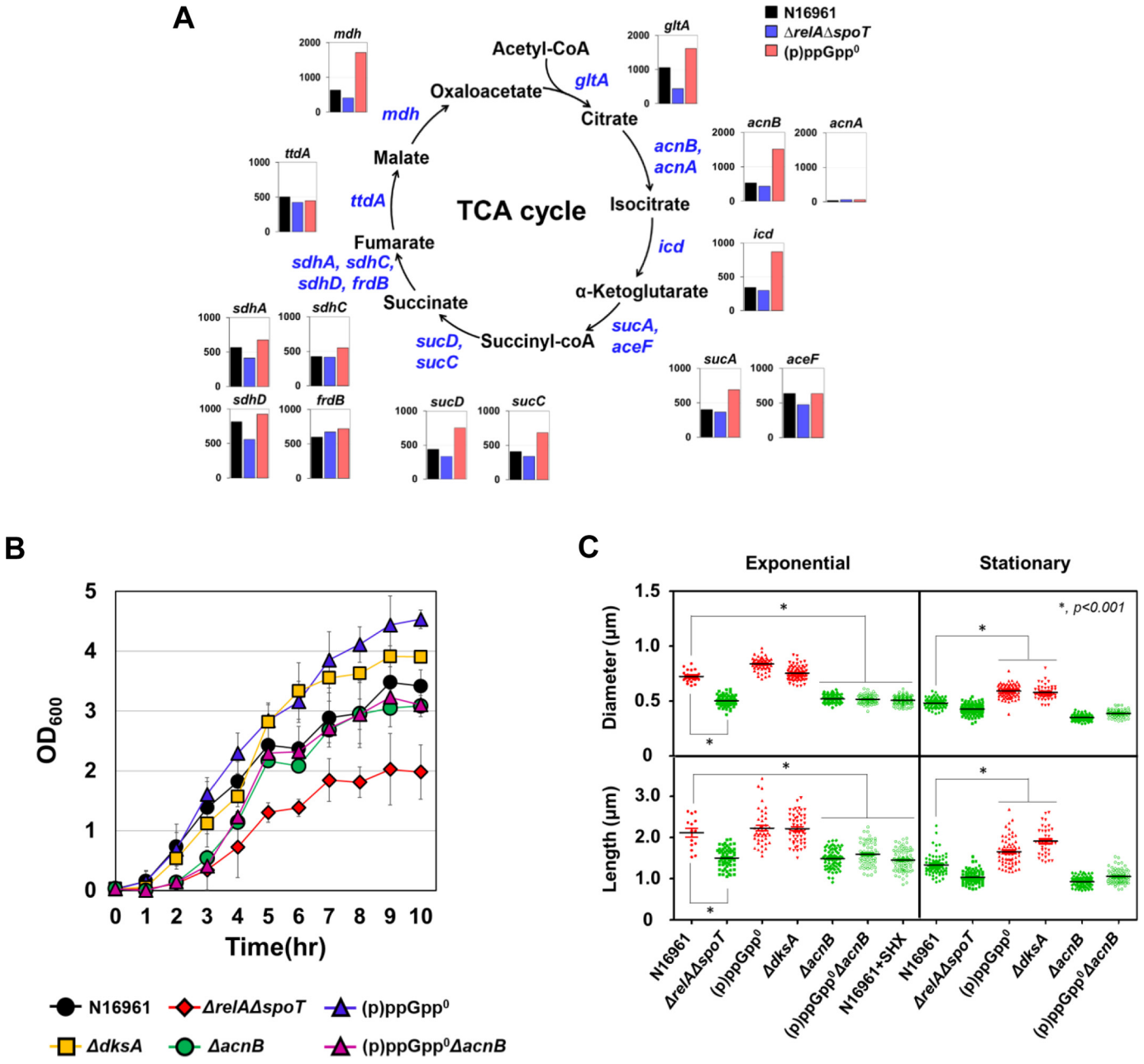

Figure 3. Effects of (p)ppGpp on central metabolism and growth of *V. cholerae* strains. *A*, RNA-sequencing analysis of TCA cycle enzymes dependent on (p)ppGpp accumulation. RNA samples extracted from three independent bacterial cultures were pooled together for the analysis. Transcripts were extracted at 16 h from bacterial cells grown under LB. Each *bar* represents the RPKM value of the transcript. *B*, bacterial cells were inoculated in LB and grown in aerobic conditions for 10 h. A_{600} values were measured every 1 h. *C*, scanning electron microscope analysis of N16961 and various (p)ppGpp-associated mutant strains grown under identical conditions as seen in Fig. 1. The plots show the distribution of diameter and length of each strain. The *solid horizontal lines* represent the geometric mean values. *, $p < 0.001$.

regulation of the *sdhA*, *sdhC*, *sdhD*, *frdB*, and *ttdA* genes (Fig. 3*A*), our RNA-sequencing results strongly suggest that TCA cycle activity is inversely regulated by intracellular (p)ppGpp concentrations.

We then asked whether the (p)ppGpp-dependent regulation of TCA cycle gene expression was reflected in bacterial growth. When wildtype N16961 was grown aerobically in LB, A_{600} values were reached at ~1.38 at 4 h post-inoculation and gradually increased up to ~3.5 for the rest of the experimental period (Fig. 3*B*). Consistent with a previous finding (21), bacterial growth was significantly retarded in the Δ*relA*Δ*spoT* mutant, which accumulates (p)ppGpp. Final A_{600} values were ~2.0. In contrast, the (p)ppGpp^0 mutant exhibited faster growth compared with N16961, and final A_{600} was reached at ~4.5 (Fig. 3*B*). Similarly, the Δ*dksA* mutant grew more vigorously, compared with N16961, further confirming that the Δ*dksA* mutant shared growth-associated phenotypes with the (p)ppGpp^0 mutant (Fig. 3*B*). To reveal the effect of *acnB* gene deletion on bacterial growth, we also monitored the growth of Δ*acnB* and (p)ppGpp^{0}Δ*acnB* mutants. Both mutants exhibited a significantly retarded growth during the early growth stage. For the first 3 h, their growth was comparable with that of the

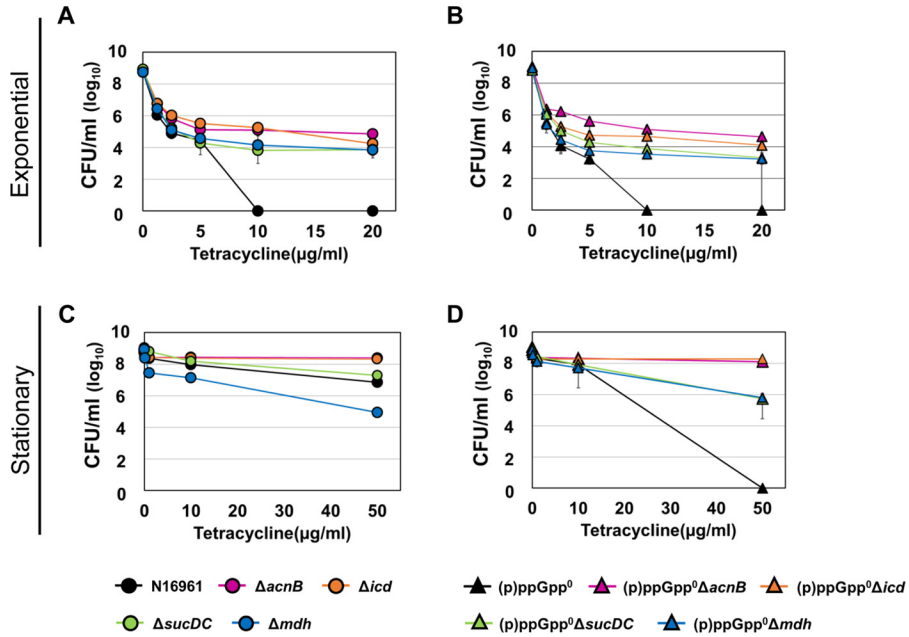

Figure 4. Effects of TCA cycle gene mutations on *V. cholerae* antibiotic tolerance. Bacterial viabilities under various Tc concentrations were measured. Each mutation indicated *below* in *different colors* was introduced in N16961 (*A* and *C*) and the (p)ppGpp^0 mutant (*B* and *D*). Bacterial strains were inoculated in LB and aerobically grown to exponential (*A* and *B*) or stationary phase (*C* and *D*). Experimental conditions were identical to those described in Fig. 1, *E* and *H*.

Δ*relA*Δ*spoT* mutant (Fig. 3*B*). Importantly, the robust growth phenotype of the (p)ppGpp^0 mutant disappeared when the *acnB* gene was additionally disrupted, further suggesting that derepressed aerobic growth of the (p)ppGpp^0 mutant was associated with increased activity of the *acnB* gene product (Fig. 3*B*).

Elevated antibiotic resistance is observed when bacterial cells exhibit a persister phenotype that is often accompanied by cell shape changes (48–50). To address this possibility, we analyzed digitized images of various bacterial strains that showed distinct antibiotic susceptibility. N16961 cells, harvested at the stationary phase and thus more resistant to antibiotics, were shorter and thinner than those harvested at the exponential phase (Fig. 3*C* and Fig. S3). Antibiotic-tolerant Δ*relA*Δ*spoT* mutant and SHX-treated N16961 cells looked thinner and shorter, regardless of when they were harvested (Fig. 3*C* and Fig. S3). In contrast, antibiotic-susceptible (p)ppGpp^0 and Δ*dksA* mutants maintained their regular curve-shaped morphotype even at the stationary phase (Fig. 3*C* and Fig. S3). These results clearly suggest that bacterial cells with reduced size are probably more resistant to antibiotic treatment. Of particular interest is that disruption of the *acnB* gene also resulted in shorter and thinner morphotypes, a phenotype observed under (p)ppGpp-accumulating conditions (Fig. 3*C* and Fig. S3). Together, these results demonstrated that (i) cell shape changes could be induced upon intracellular (p)ppGpp accumulation or metabolic alterations by *acnB* gene mutation and (ii) such changes are closely related to bacterial responses to antibiotic treatment.

Other TCA cycle mutants also exhibit increased antibiotic tolerance

To see whether other TCA cycle mutants also exhibit phenotypes similar to that of the *acnB* mutant, we additionally constructed in-frame deletion mutants of TCA cycle enzymes (Δ*icd*, Δ*sucDC*, and Δ*mdh*) in both wildtype N16961 and (p)ppGpp^0 mutant background and monitored their responses to the Tc treatment. As shown in Fig. 4, TCA cycle mutants were also found to be resistant to Tc. The Δ*icd* mutant showed the most similar resistance to the Δ*acnB* mutant, whereas the remaining two mutants (Δ*sucDC* and Δ*mdh*) showed lower resistance (Fig. 4, *A* and *C*). Importantly, when each of these mutations was introduced in the antibiotic-sensitive (p)ppGpp^0 mutant, antibiotic resistance was restored (Fig. 4, *B* and *D*). Compared with the (p)ppGpp^0 mutant, (p)ppGpp^{0}Δ*acnB* and (p)ppGpp^{0}Δ*icd* mutants maintained their viabilities at ~10^8 cells/ml following 4-h Tc treatment at 50 μg/ml. The (p)ppGpp^{0}Δ*sucDC* and (p)ppGpp^{0}Δ*mdh* survived at ~10^6 cells/ml. Taken together, these results suggest that disruptions of the TCA cycle function due to the mutation of either the *acnB* gene or other constituting genes affected antibiotic resistance in *V. cholerae*. Our results also show that ablation of the *acnB* or *icd* gene, whose products mediate early steps of the TCA cycle, produced a more profound effect on bacterial responses to antibiotic stresses.

Antibiotic-mediated bacterial killing occurs only in the presence of molecular oxygen and iron

Our results so far showed that (i) expression of TCA cycle genes, such as *acnB*, *icd*, and *mdh*, was highly induced in the antibiotic-susceptible (p)ppGpp^0 mutant, (ii) antibiotic-mediated bacterial killing was reduced in each of these TCA cycle mutants, and (iii) when (p)ppGpp was accumulated, bacterial cells shrank and became antibiotic-tolerant. These findings led us to hypothesize that (p)ppGpp accumulation results in metabolic slowdown, rendering bacterial cells unresponsive to antibiotics. To explore whether active metabolism, possibly fueled by aerobic respiration, is necessary for antibiotic-mediated bac-

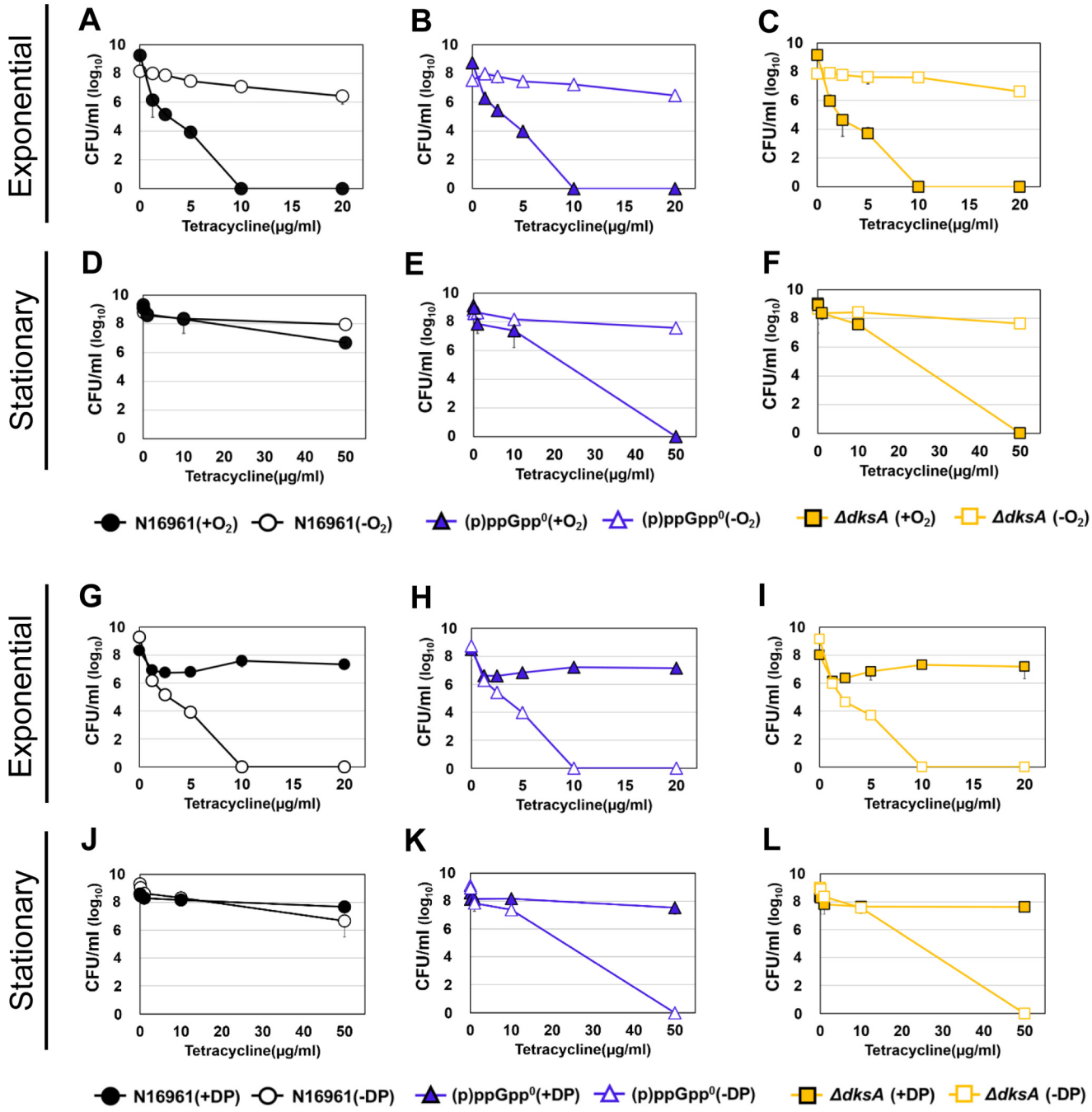

Figure 5. Recovery of tetracycline resistance of (p)ppGpp-deficient strains under anaerobic and iron-deplete conditions. *A–F*, tetracycline resistance of N16961 (*circles*), (p)ppGpp^0 mutant (*triangles*), and Δ*dksA* mutant (*squares*) strains under anaerobic conditions. Wildtype N16961 and various (p)ppGpp-associated mutant strains were inoculated in LB and aerobically grown to each growth stage. Aliquots of each culture were resuspended in several concentrations of antibiotic-containing LB broth and incubated for 4 h in anaerobic conditions. Each aliquot was sampled and 10-fold serially diluted to assess the number of cfu. *G–L*, tetracycline resistance of N16961 and (p)ppGpp-deficient mutant strains under iron-depleted conditions. Aliquots of each culture were resuspended in several concentrations of tetracycline-containing LB supplemented with 2,2′-dipyridyl, sampled at 4 h post-inoculation, and serially diluted for cfu counting.

terial killing, we compared bacterial responses under aerobic *versus* anaerobic environments. Exponential-phase N16961 cells, which were found to be antibiotic-sensitive, maintained their viability when further grown for 4 h anaerobically with Tc (Fig. 5*A*). Anerobiosis also provided an additional protective effect (>10-fold) on stationary-phase N16961 cells against 50 μg/ml Tc (Fig. 5*D*). Likewise, only marginal viability loss was observed upon treatment with Tc in two antibiotic-sensitive mutants, (p)ppGpp^0 (Fig. 5, *B* and *E*) and Δ*dksA* (Fig. 5, *C* and *F*), under strict anaerobic environments. These results demonstrated that antibiotic-mediated bacterial killing occurred only during aerobic growth.

Hydroxyl radical (OH$^\bullet$), the most bactericidal ROS, was reported to be produced during antibiotic treatments in large quantities (43). Because its production is catalyzed by the iron-mediated Fenton reaction (51, 52), we next examined how bac-

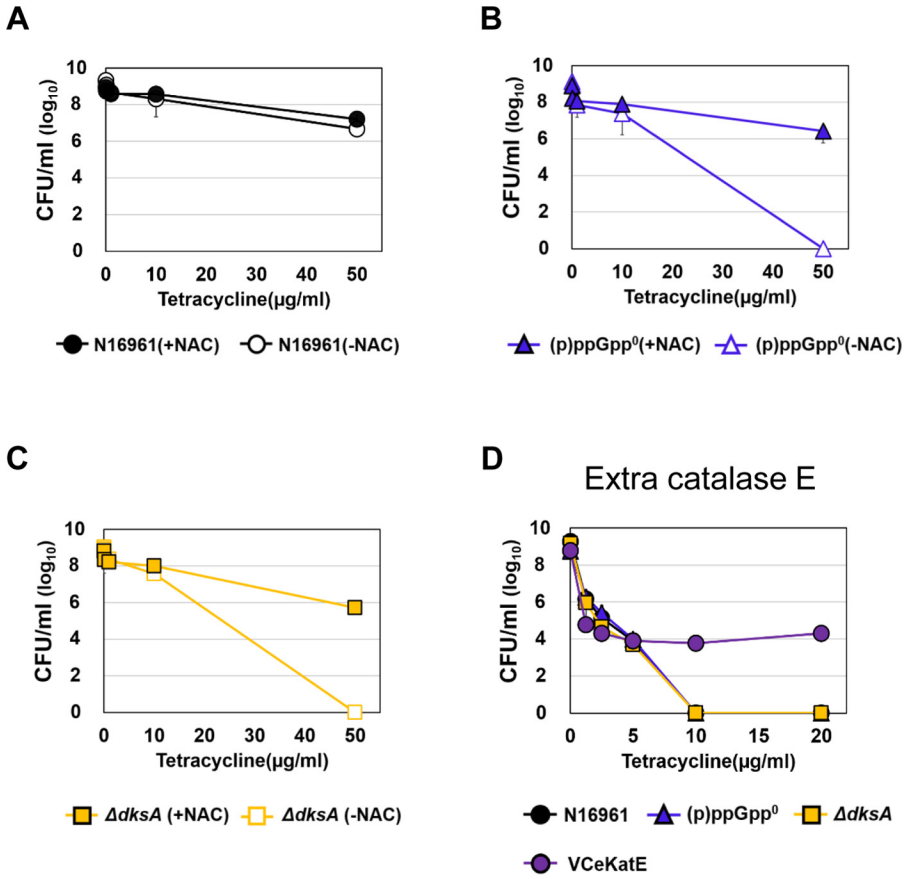

Figure 6. Effects of an ROS scavenger and additional catalase production on bacterial tetracycline resistance. *A–C*, tetracycline resistance of N16961 and (p)ppGpp-deficient mutant strains under ROS-scavenger treatment. Aliquots of each culture were resuspended in several concentrations of tetracycline-containing LB supplemented with 5 mM NAC, respectively, sampled at 4 h post-inoculation, and serially diluted for cfu counting. *D*, bacterial viability of (p)ppGpp-deficient mutants and eKatE-producing N16961 (N16961::pVIK112+*eKatE*) under the tetracycline treatment.

terial responses were altered under iron-depleted conditions. To this end, bacterial strains were treated with Tc in the presence of 2,2′-dipyridyl, an iron chelator (43). As shown in Fig. 5 (*G–L*), bacterial strains remained viable under iron-deficient conditions after being treated with as high as 50 μg/ml Tc for 4 h (Fig. 5, *J–L*). Again, two antibiotic-vulnerable mutants and exponential-phase N16961 cells were completely killed by the same treatment in iron-sufficient LB. We then examined whether bacterial killing was alleviated by co-treatment with *N*-acetylcysteine (NAC), an ROS scavenger. Bacterial survival was substantially restored when antibiotic-sensitive (p)ppGpp^0 and Δ*dksA* mutants were co-treated with 5 mM NAC (Fig. 6, *B* and *C*). As expected, NAC treatment exerted no protective effects on stationary-phase N16961 cells already resistant to Tc treatment (Fig. 6*A*). Together, these results indicated that (i) iron availability determined bacterial survival during antibiotic stress and (ii) ROS, produced aerobically during antibiotic treatment, were responsible for bacterial killing.

Consistent with these results, post-antibiotic ROS production was indeed increased in two antibiotic-sensitive mutants (Fig. 7). When treated with Tc for 1 h, ROS-specific fluorescent signals increased ~100- and ~1,000-fold in (p)ppGpp^0 and Δ*dksA* mutant, respectively. In contrast, fluorescent signals increased only ~10-fold in stationary-phase N16961 cells and (p)ppGpp-accumulating Δ*relA*Δ*spoT* mutant (Fig. 7). It is of particular importance that post-antibiotic ROS production was not detected in the Δ*acnB* single and (p)ppGpp^{0}Δ*acnB* quadruple mutant (Fig. 7), thereby further demonstrating that the recovered antibiotic resistance by *acnB* gene deletion is associated with the lack of ROS production.

Recently, we reported a recombinant N16961 strain that harbored an *eKatE* gene encoding a robust catalase (53). The *eKatE* gene is derived from a commensal *Escherichia coli* strain, and this strain was found to be resistant to 2 mM H_2O_2 concentration. This strain, when harvested at the exponential phase, developed clear resistance to Tc treatment. Whereas the control N16961 strain perished completely during the same treatment, ~10^4 cells remained viable (Fig. 6*D*). This result further supports our finding that ROS resistance can help with antibiotic tolerance.

Larger amounts of intracellular free iron are present in SR-negative mutants

Next, we sought to further elucidate mechanisms by which (p)ppGpp regulates iron-dependent ROS production during aerobic antibiotic treatment. Table 1 lists the top five genes, expression of which was highly induced in the antibiotic-susceptible (p)ppGpp^0 mutant, as normalized with that of each counterpart in the antibiotic-tolerant Δ*relA*Δ*spoT* mutant. Among these are genes encoding heme transport protein (*hutA*), enterobactin receptor protein (*irgA*), and periplasmic Fe(III) ABC transporter substrate–binding protein (*fbpA*).

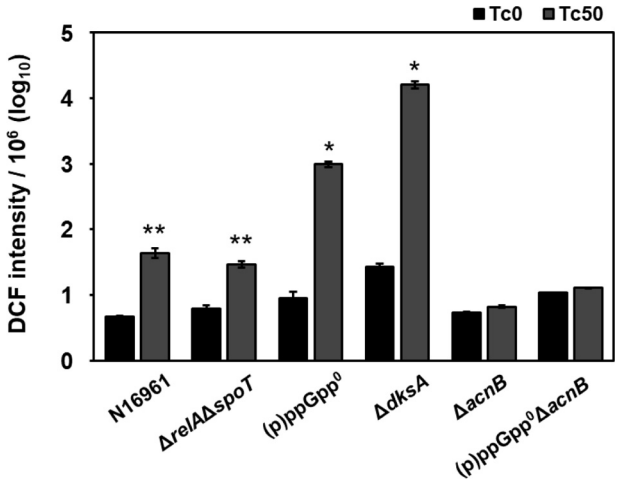

Figure 7. Antibiotic-induced ROS production in (p)ppGpp-deficient mutant strains. Bacterial strains indicated at the *bottom* were treated with 50 μg/ml Tc for 1 h (*gray bars*) or left untreated (*black bars*). Following treatment, bacterial cells were stained with 50 μM DCF for 30 min to measure intracellular ROS levels. DCF intensity was normalized with bacterial cfu and is displayed in logarithmic scale. *, $p < 0.0001$ *versus* values of untreated groups. **, $p < 0.001$ *versus* values of untreated groups. *Error bars*, S.D.

Because these proteins are involved in iron acquisition, these RNA-sequencing data strongly suggest that the iron uptake system may be inversely regulated by intracellular (p)ppGpp levels. Consistent with this notion, production of FbpA protein was markedly increased in two SR-negative mutants, whereas its production was not detected in the (p)ppGpp-accumulating Δ*relA*Δ*spoT* mutant (Fig. 8*A*).

To understand the role of FbpA in iron uptake and antibiotic tolerance, we introduced an in-frame deletion of the *fbpA* gene in the N16961, (p)ppGpp^0, and Δ*dksA* mutants (Fig. S4). Bacterial growth was not affected by *fbpA* gene deletion (data not shown). When we measured intracellular free iron concentrations by whole-cell EPR spectrometry, iron-specific signals were invariably decreased in the N16961, (p)ppGpp^0, or Δ*dksA* strains when the *fbpA* gene was inactivated (Fig. 8*B*). The (p)ppGpp^{0}Δ*fbpA* quadruple and Δ*dksA*Δ*fbpA* double mutants contained ~2-fold and ~3.3-fold decreased levels of free iron, respectively, when compared with their parental mutants (Fig. 8*B*). These results showed that FbpA protein played an important role in iron uptake in *V. cholerae*. It is of particular interest that substantially increased amounts of free iron were detected in two antibiotic-susceptible mutants, as compared with N16961 (Fig. 8*B*). Together, these results clearly demonstrated that the iron import system was suppressed by (p)ppGpp accumulation, and this down-regulation could contribute to reducing the level of intracellular free iron, the crucial source of hydroxyl radical ($OH^{\bullet}$) formation.

In line with these findings, bacterial survival under Tc treatment was significantly increased in Δ*fbpA* mutants (Fig. 8, *C–H*). When exponential-phase cells were used for treatment, bacterial viability of up to ~10^4-fold was recovered in Δ*fbpA*, (p)ppGpp^{0}Δ*fbpA*, and Δ*dksA*Δ*fbpA* mutants compared with each of their background strains (Fig. 8, *C*, *E*, and *G*). Moreover, (p)ppGpp^{0}Δ*fbpA* and Δ*dksA*Δ*fbpA* mutants, harvested at the stationary stage, also exhibited Tc resistance (Fig. 8, *F* and *H*).

Discussion

Cholera is characterized by CT-induced profuse watery diarrhea. Rapid loss of body fluids often leads to fatal dehydration (54–56). Although up to 80% of cholera patients can be treated with oral rehydration therapy, annual deaths up to 120,000 are reported (81). Mortality includes victims who fail to receive immediate interventions and young patients with immature stomach function (82). These cases apparently need prompt antibiotic treatment to reduce the volume of diarrhea and kill the causative pathogen, *V. cholerae*. Treating cholera patients with antibiotics, however, has been a challenge due to the increased emergence of antibiotic-tolerant *V. cholerae* strains (16–20, 57).

In this study, we proposed that SR, a conserved bacterial stress response mechanism, regulates antibiotic tolerance in *V. cholerae* via mechanisms that eventually suppress ROS production. SR controls metabolic activity and intracellular iron level, both of which affect bacterial growth and thereby antibiotic-induced ROS generation. Our successful demonstration on this important issue was made possible by the availability of the Δ*relA*Δ*spoT* double mutant that spontaneously accumulates intracellular (p)ppGpp. Whereas (p)ppGpp-null phenotypes have been well-documented in various bacterial species (21, 41, 58, 59), cellular phenotypes induced by natural (p)ppGpp accumulation have not been clearly described. The (p)ppGpp-accumulating Δ*relA*Δ*spoT* mutant (i) metabolized slowly, (ii) exhibited a smaller cell-size phenotype, and (iii) produced significantly decreased levels of FbpA protein involved in iron acquisition. All of these phenotypes were invariably reversed in (p)ppGpp^0 and Δ*dksA* mutants, determined to be antibiotic-susceptible. Among these phenotypes, FbpA-mediated iron metabolism provided us with a clue that helped us to precisely elucidate the role of ROS in antibiotic-mediated bacterial killing.

V. cholerae is an enteric pathogen that is transmitted through the fecal-oral route. The toxigenic *V. cholerae* is able to rapidly spread through bacterial shedding by evoking deadly diarrhea. It passes through the esophagus and comes into contact with the acid environment of the stomach, to which *V. cholerae* is known to be susceptible. Moreover, *V. cholerae* colonizes the small intestine, where it must compete with diverse species of commensal microbes for nutrients (60). To overcome such unfavorable conditions, it is highly likely that SR is activated in *V. cholerae* inside the host intestine. Consistent with this idea, our previous work (21) demonstrated that (i) SR-defective mutants are incapable of colonizing mouse intestine and (ii) the (p)ppGpp-accumulating Δ*relA*Δ*spoT* mutant produces a markedly increased level of CT. We therefore proposed that strains that survive and shed out to the environments may have active SR and thereby be more able to infect subsequent hosts and overcome antibiotic stresses. To further validate this hypothesis, it will be important to compare SR activity status in pandemic *versus* non-virulent environmental strains.

Our results demonstrated that (p)ppGpp, when accumulated, down-regulated expression of many TCA cycle genes, including *acnB*. Not surprisingly, bacterial metabolism and growth were reported to be suppressed by SR in diverse bacte-

Table 1
List of genes showing the expression significantly increased in (p)ppGpp^0 compared with Δ*relA*Δ*spoT* mutant

Gene no.	Δ*relA*Δ*spoT*	(p)ppGpp^0	(p)ppGpp^0/Δ*relA*Δ*spoT*	Product
VCA0819	129.41	2612.98	20.19	Co-chaperonin GroES
VC2664	217.95	3203.18	14.70	Molecular chaperone GroEL
VCA0576	134.48	1804.06	13.42	Heme transport protein HutA
VC0475	101.92	1343.82	13.19	Enterobactin receptor protein IrgA
VC0608	219.09	2653.88	12.11	Fe(III) ABC transporter substrate–binding protein FbpA

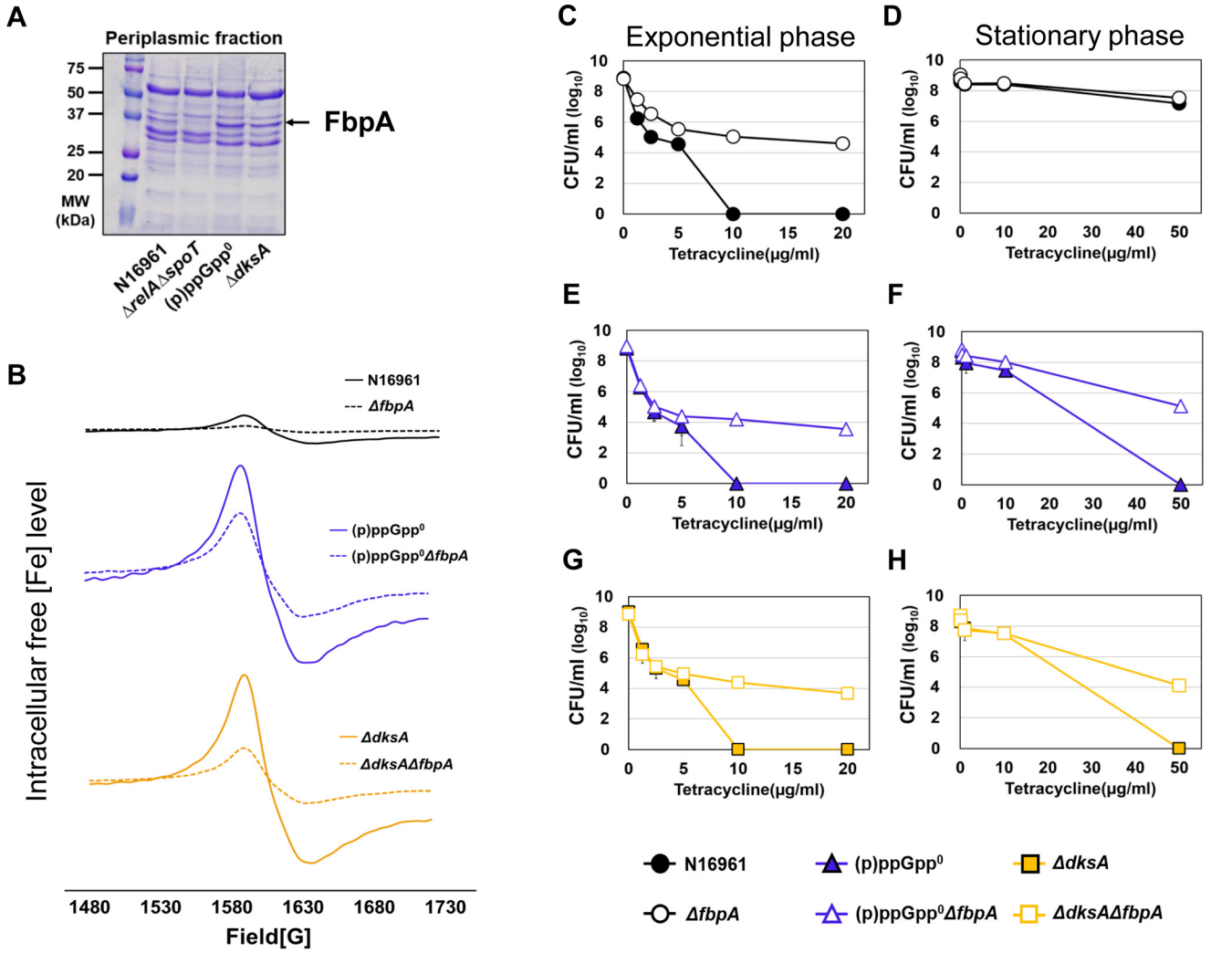

Figure 8. Effects of *fbpA* gene deletion on tetracycline resistance and the levels of intracellular free iron in *V. cholerae*. *A*, SDS-PAGE analysis of periplasmic fractions in wildtype and (p)ppGpp-associated mutants. Periplasmic fraction was extracted at 16 h from bacterial cells grown under LB and loaded onto SDS-PAGE. *B*, the levels of intracellular unincorporated iron in N16961 and (p)ppGpp-deficient mutant and *fbpA*-deletion mutant strains were measured by whole-cell electron paramagnetic resonance (EPR) analysis. The EPR peaks represent the content of total free iron converted to ferric form. *C–H*, bacterial viability of the (p)ppGpp-deficient mutant and *fbpA*-deletion mutants under tetracycline treatment.

rial species (25, 61, 62). Studies also suggested that (p)ppGpp-mediated regulation participated in bacterial persister formations by mechanisms that involved toxin-antitoxin modules (63, 64). Bacterial persisters are transient phenotypic variants that are stochastically induced within a subset of cells in a given population (64). Persister cells, in general, are more tolerant of antibiotic treatments (65). Ronayne *et al.* (48) showed that *E. coli* cells undergo cell elongation during the acquisition of a persister phenotype. In contrast, *V. cholerae* cells, incubated for a long time in nutrient-poor media, were shown to be smaller in size when compared with normal state cells (50), suggesting that the potential persister-like phenotype may be achieved in a distinct manner in *V. cholerae*. Our results showed that the (p)ppGpp-accumulating Δ*relA*Δ*spoT* mutant and SHX-treated N16961 cells were thinner and shorter. Interestingly, reduced cell size was also observed in the Δ*acnB* single mutant. These results indicated that cell shape change and a resultant increase in antibiotic tolerance ensued from (p)ppGpp accumulation or *acnB* gene deletion in *V. cholerae* and presented a new question as to which of these two cellular processes was the primary cause of the phenotype. Because a similar cell-size reduction was also detected in the (p)ppGpp^{0}Δ*acnB* mutant cells, we postulate that *acnB* gene deletion is a necessary and sufficient condition for the phenotype. Likewise, cell size reduction in the

Δ*relA*Δ*spoT* mutant was probably induced by suppressed aconitase activity, not directly by (p)ppGpp accumulation. Cell biological features need to be further explored in terms of how inactive metabolism can lead to changes in cell shape.

Periplasmic Fe(III) ABC transporter substrate–binding protein, encoded by *fbpA*, was highly produced in antibiotic-susceptible (p)ppGpp^0 and Δ*dksA* mutants. More importantly, EPR analysis clearly showed that intracellular free iron was concomitantly increased in these two mutants. Like other bacterial species, *V. cholerae* requires iron for growth and possesses a variety of iron uptake systems (66). The iron acquisition systems in *V. cholerae* involve synthesis, secretion, and uptake of a range of siderophore molecules, such as vibriobactin (67), enterobactin (68, 69), and ferrichrome (67, 70). In addition, *V. cholerae* possesses *feo* and *fbp* gene clusters encoding systems for the acquisition of ferrous and ferric iron, respectively (66). The Fbp system is a periplasmic binding protein–dependent ABC transport system and consists of three genes, *fbpA* (VC0608), *fbpB* (VC0609), and *fbpC* (VC0610). The *fbpB* and *fbpC* encode membrane-spanning proteins forming a pore across the cell membrane and ATP binding proteins, respectively. The *fbpA* encodes a substrate-binding protein that carries ferric iron to the membrane-spanning proteins. Studies indicate that the potential Fur box (ferric uptake regulator–binding motif) exists in the promoter region of the *fbpABC* operon (66, 71), suggesting that expression of the operon is highly induced under iron-deficient conditions. However, in our experiments, bacterial strains were grown in LB, considered to be a nutrient-rich medium. It was of particular interest to us that the Fur protein is inactivated by the presence of ROS (72). ROS oxidizes Fe^{2+}, a co-factor of Fur, converting active Fur into an inactive apo-form. Therefore, one possible explanation for the antibiotic-mediated bacterial killing in the antibiotic-susceptible (p)ppGpp^0 and Δ*dksA* mutants would be that ROS produced during derepressed aerobic growth stimulated FbpA-mediated iron uptake, which in turn amplified further ROS production. In support of this idea, the Δ*relA*Δ*spoT* mutant that grew very slowly produced undetectable levels of FbpA protein. Furthermore, we also found that FbpA production was reduced in the Δ*acnB* mutant that exhibited a slow growth phenotype (data not shown).

In our experiments, the first-line drugs for treating cholera patients, tetracycline, erythromycin, and chloramphenicol, were used. We found that SR-deficient mutants of *V. cholerae* completely lost their viability as the antibiotic concentration increased. Interestingly, however, the antibiotics that turned out to be very effective at killing *V. cholerae* strains are commonly known as bacteriostatic. Although it is still debatable how to classify antibiotics as bacteriostatic or bactericidal based on their *in vitro* test results, recent studies described their differences based on their effects on bacterial metabolism. Lobritz *et al.* (44) found that bacteriostatic and bactericidal have opposing effects on bacterial respiration in *E. coli* and *Staphylococcus aureus*. They demonstrated that bacteriostatic antibiotics, such as tetracycline, chloramphenicol, and erythromycin, decelerate cellular respiration, whereas bactericidal antibiotics accelerate basal respiration and lead to the production of ROS as a by-product. On the other hand, we found that bacteriostatic antibiotics killed bacteria and produced deleterious ROS. Interestingly, in another study, the antibiotics that did not trigger SOS responses in *E. coli* caused SOS responses in *V. cholerae* (73). SOS stress responses were activated when exogenous and endogenous triggers provoked DNA damage, and some antibiotics act as exogenous triggers that stimulate ROS production, the crucial weapon of DNA disruption. Aminoglycosides, tetracycline, and chloramphenicol induce SOS responses in *V. cholerae*, unlike *E. coli*, and this result suggests the possibility that these antibiotics have more deleterious effects on *V. cholerae*. Taken together, our results suggest that effects of bacteriostatic and bactericidal antibiotics on bacteria vary from species to species.

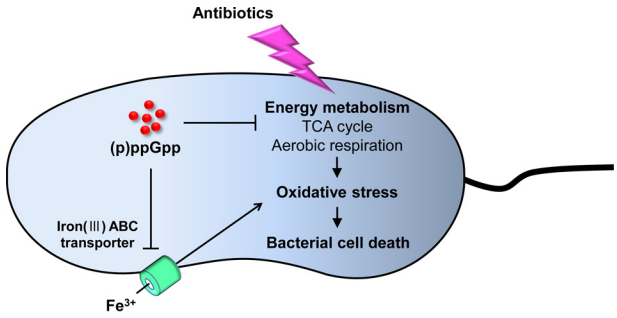

Figure 9. Summary of (p)ppGpp-mediated regulation of antibiotic resistance in *V. cholerae*. Antibiotic treatment stimulates ROS production by hyperactivating bacterial central metabolism. The released ROS leads to damage of intracellular DNA, proteins, and lipids, which results in cell death. However, (p)ppGpp negatively regulates TCA cycle and aerobic respiration. The down-regulation of aerobic respiration can reduce oxidative stress and eventually prevent cell death. The (p)ppGpp can maximize this effect by restricting free iron uptake from the iron-transporting system.

In conclusion, our results revealed that bacterial SR regulates antibiotic tolerance by modulating ROS production. Central metabolism and iron transport systems are subject to (p)ppGpp-mediated regulation (summarized in Fig. 9). When (p)ppGpp is accumulated, the TCA cycle is down-regulated to slow down bacterial growth. At the same time, FbpA-mediated iron uptake is also suppressed in (p)ppGpp-accumulating cells. These dual cellular events both contribute to physiological changes resulting in metabolic slowdown and therefore antibiotic-tolerant states. Bacterial SR has been a target to be inhibited. Chemical compounds that can suppress (p)ppGpp production, such as relacin (74) and iMAC (75), can potentially be used as antibiotic adjuvants. We anticipate that experimental data provided in the current study will stimulate future investigations that eventually help us come up with better strategies to combat bacterial infections, including one by the deadly enteric pathogen *V. cholerae*.

Experimental procedures

Bacterial strains and growth conditions

All of the bacterial strains and plasmids used in this study are listed in Table 2. Bacterial cultures were grown in LB (1% (w/v) tryptone, 0.5% (w/v) yeast extract, and 1% (w/v) sodium chloride) at 37 °C, and antibiotics were used at the following concentrations: streptomycin (Duchefa), 200 μg/ml; ampicillin (Sigma), 50 μg/ml; kanamycin (Duchefa), 50 μg/ml. All bacterial single colonies on LB plates were picked and inoculated in LB broth for precultures and grown overnight. Precultures were diluted 100-fold in fresh LB broth for subculture and incu-

Table 2
Bacterial strains and plasmids used in this study

Strains and plasmids	Relevant characteristic	Source
***V. cholerae* strains**		
N16961	Wildtype, O1 serogroup, biotype El Tor	Laboratory collection
Δ*acnB*	N16961, *acnB* deleted	This study
Δ*dksA*	N16961, *dksA* deleted	This study
Δ*icd*	N16961, *icd* deleted	This study
Δ*sucDC*	N16961, *sucDC* deleted	This study
Δ*mdh*	N16961, *mdh* deleted	This study
Δ*fbpA*	N16961, *fbpA* deleted	This study
Δ*dksA*Δ*fbpA*	N16961, *dksA* and *fbpA* deleted	This study
Δ*relA*Δ*spoT*	N16961, *relA* and *spoT* deleted	Ref. 21
(p)ppGpp^0	N16961, *relA*, *relV*, and *spoT* deleted	Ref. 21
(p)ppGpp^{0}Δ*acnB*	N16961, *relA*, *relV*, *spoT*, and *acnB* deleted	This study
(p)ppGpp^{0}Δ*icd*	N16961, *relA*, *relV*, *spoT*, and *icd* deleted	This study
(p)ppGpp^{0}Δ*sucDC*	N16961, *relA*, *relV*, *spoT*, and *sucDC* deleted	This study
(p)ppGpp^{0}Δ*mdh*	N16961, *relA*, *relV*, *spoT*, and *mdh* deleted	This study
(p)ppGpp^{0}Δ*fbpA*	N16961, *relA*, *relV*, *spoT*, and *fbpA* deleted	This study
N16961::pVIK112+*eKatE*		Ref. 53
***E. coli* strains**		
SM10/λpir	Km^r *thi-1 thr leu tonA lacY supE recA*::RP4–2-Tc::Mu *pir*$^+$, for conjugal transfer	Laboratory collection
Plasmids		
pBAD24	Amp^r, cloning vector	Laboratory collection
pCVD442	*sacB* suicide vector from plasmid pUM24	Laboratory collection
pTnKGL3	Suicide vector bearing TnKGL3, Cm^r, Km^r	Laboratory collection

bated at 37 °C and 220 rpm. The incubation time was dependent on experimental procedures.

Antibiotic tolerance assay

All antibiotic tolerance assays in this study were performed as described previously with a few modifications (41). For bacterial drug experiments, we used tetracycline (Sigma), erythromycin (Sigma), chloramphenicol (Sigma).

Exponential-phase bacteria—Bacteria from precultures were diluted 100-fold in LB broth and grown shaking at 37 °C until the growth reached A_{600} 0.5. 5 mM serine hydroxamate (Sigma) was added to some of the cultures after 1 h of growth and further incubated for 1 h. Aliquots were then resuspended in serial diluted antibiotic-LB to A_{600} 0.05 and incubated statically for 4 h. The cfu were measured by serial dilution of individual aliquots on LB plates for statistical testing.

Stationary-phase bacteria—Overnight subcultures (16 h) were resuspended in serial diluted antibiotic-LB aliquots to A_{600} 0.3 and statically incubated for 4 h. The survival rate of individual aliquots was also measured by viable cell counting.

Determination of intracellular (p)ppGpp concentration by TLC

Intracellular ppGpp concentration was measured as described previously with a few modifications (22). To detect intracellular (p)ppGpp, bacterial cells were grown aerobically with 100 μCi/ml [^{32}P]orthophosphate (PerkinElmer Life Sciences) at each growth phase. The bacterial cell cultures were extracted with cold 10 mM Tris-HCl buffer (pH 8.0). After centrifugation to remove the cell supernatant, cell pellets were resuspended with cold 10 mM Tris-HCl buffer and 19 M formic acid and then freeze-thawed for three cycles. After centrifugation to remove cell debris, cell supernatants were spotted on PEI cellulose F TLC plates (Merck). The TLC plates were developed in 1.5 M KH_2PO_4 buffer (pH 3.4) in a humidified chamber and imaged with autoradiography.

Construction of in-frame deletion mutants

V. cholerae mutants were created by allele replacement, as described previously (21, 76). To induce mutation, 500-bp flanking sequences located at both ends of the ORF were amplified by PCR with the primers listed in Table 3. The primers used to amplify each flanking region were carried by restriction enzyme sites that were located in multiple cloning sites of pCVD442 suicide vectors. The purified forward flanking sequences were ligated in pCVD442 vector with T4 ligase, and extracted vectors were transformed to heat-shock competent cells, SM10/λpir strains. The transformed cells were selected on LB plates containing 100 μg/ml ampicillin, and cloning vectors were purified from single survival colonies, following recombination of another flanking sequence going through the same steps to transformation. The SM10/λpir strains with cloned vectors and *V. cholerae* recipient strains were mixed at a ratio of 3:1 onto LB plates and incubated for 6 h at 37 °C. The mixed pool was suspended in fresh LB broth and spread on LB plates containing 200 μg/ml streptomycin or 100 μg/ml ampicillin for the first step in allelic exchange. After overnight culture, for plasmid excision from the chromosome by second cross-over, single colonies were selected and streaked on LB plates with 8% sucrose and 200 μg/ml streptomycin without NaCl. Screening of in-frame deletion sites for each colony was preceded by PCR to identify the desired allele with primers that contained flanking sequences and ORF.

Construction of a random Tn-insertion mutant library

A Tn-inserted mutant library was constructed by using the mariner-based Tn, TnKGL3, which contains a kanamycin resistance marker. Tn mutagenesis of Δ*relA*Δ*relV*Δ*spoT* (*i.e.* (p)ppGpp^0) mutant was performed with SM10/λpir, which carries the TnKGL3. SM10/λpir strains and the *V. cholerae* recipient strain were mixed at a ratio of 2:1 onto LB plates and incubated for 6 h at 37 °C. The mixed pool was suspended with fresh LB broth and spread on LB plates containing 200 μg/ml strep-

Table 3
Primers used in this study

Gene name	Direction[a]	Primer sequence (5′–3′)[a]
Cloning		
Δ*acnB* left	Forward	GCAAGCATGCAAACCTCGTTTACCGTTACC
Δ*acnB* left	Reverse	CTCTGAGCTCGACTTTTTCCTCTCATTGCG
Δ*acnB* right	Forward	TTGCGAGCTCGCAGAGTGATTGAATCCTCT
Δ*acnB* right	Reverse	GCGACCCGGGATTTTGAATAAAGCTTTGCC
Δ*icd* left	Forward	TATTGCATGCTGGCTTAAAGTGTCATAAGG
Δ*icd* left	Reverse	GTCTAAACTAGAGAACTTTCCCTATCTGTTCT
Δ*icd* right	Forward	TAGGGAAAGTTCTCTAGTTTAGACACCAAAAC
Δ*icd* right	Reverse	ATGTGCATGCATACGTTCGTCCTATTGACT
Δ*sucDC* left	Forward	TATTGCATGCGTGATTTGCTCGCGATTAGC
Δ*sucDC* left	Reverse	TGGAACAACACATCTACCGCGATTACTTACTC
Δ*sucDC* right	Forward	AATCGCGGTAGATGTGTTGTTCCATTTGTTTA
Δ*sucDC* right	Reverse	ATCTGAGCTCATACCTTGAGTTTGGCGCAA
Δ*mdh* left	Forward	AGTTGCATGCGCGATACTTTGGATTGGTTG
Δ*mdh* left	Reverse	ATCGATTGTCGACGTAAATCTCCTTGAGAGTA
Δ*mdh* right	Forward	AGGAGATTTACGTCGACAATCGATTCAAGCAT
Δ*mdh* right	Reverse	ATTAGAGCTCTGAACCAATCACTAGCGCCG
Δ*fbpA* left	Forward	TGCTGCATGCTTTTAGTGTGTAAAACCACT
Δ*fbpA* left	Reverse	CGGCGAGCTCTGTATTATAGGAATGTTCAA
Δ*fbpA* right	Forward	TCGCGAGCTCGTAAAATCAGGGGTATAACG
Δ*fbpA* right	Reverse	CGCGCCCGGGATACACATAAGGATAAAGTA
Arbitrary PCR		
KGL3-Mar1, 1 round	Forward	GGGAATCATTTGAAGGTTGGT
Arb1, 1 round	Reverse	GGCCACGCGTCGACTAGTACNNNNNNNNNNGATAT
Arb6, 1 round	Reverse	GGCCACGCGTCGACTAGTACNNNNNNNNNNACGCC
KGL3-Mar2, 2 round	Forward	TAGCGACGCCATCTATGTGTC
Arb2, 2 round	Reverse	GGCCACGCGTCGACTAGTAC

[a] Restriction enzyme recognition sequences are underlined.

tomycin, 100 μg/ml kanamycin and incubated overnight. The survival bacterial pool was harvested in LB broth and diluted in LB aliquots containing 50 μg/ml tetracycline to A_{600} 0.3 and statically incubated for 4 h. The whole bacterial cells of each aliquot were recruited for centrifugation and resuspended again in LB aliquots containing 50 μg/ml tetracycline and incubated for 4 h. These procedures were repeated three times, and final aliquots were partially spread on LB plates containing streptomycin and kanamycin. The surviving bacterial colonies were collected into a library, and the Tn-insertion site for each mutant was determined by arbitrary PCR. The first round of arbitrary PCR was performed by the transposon TnKGL3-specific primer Mar1 and two random primers, Arb1 and Arb6. The following second round of PCR proceeded with Mar2 and Arb2, by using the first-round PCR products for templates. The PCR products were sequenced using the primer Mar2. The Tn-inserted locations were identified by comparison with the public database of the *V. cholerae* genome sequence.

Scanning electron microscopy analysis

Characterization of bacterial cell morphology and size were visualized with scanning electron microscopy, following procedures described previously (77). Briefly, for the sample preparation, bacterial cell cultures were fixed with PBS containing 2% glutaraldehyde and 0.1% paraformaldehyde for 2 h and stained with 1% OsO_4. Samples were then coated with gold by an ion sputter (IB-3, Eiko, Japan) and examined with a scanning electron microscope (FE SEM S-800, Hitachi, Japan) at an acceleration voltage of 20 kV. Images were processed with ESCAN 4000 software (Bummi Universe Co., Ltd., Seoul, Korea). For measuring the cell length and diameter, more than 100 straight-lined cells were randomly chosen from the digitized scanning electron microscopy images, and the distance between the two ends was automatically calculated.

RNA-sequencing analysis

Bacterial cultures grown in LB were harvested at 16 h post-inoculation. Aliquots of each culture ($n = 3$) were pooled together in one tube for RNA analysis. To extract high-quality bacterial RNA, an RNeasy Protect kit (Qiagen) was used with an RNeasy minikit (Qiagen) following the manufacturer's protocol. The quantity and quality of total RNA were evaluated using RNA electropherograms (Agilent 2100 Bioanalyzer, Agilent Technologies, Waldbroon, Germany) and by assessing the RNA integrity number. From each sample with an RNA integrity number value greater than 8.0, 8 μg of the total RNA was used as a starting material and treated with the MICROBExpress™ mRNA enrichment kit (Invitrogen). The resulting mRNA samples were processed for the sequencing libraries using Illumina mRNA-Seq sample preparation kit (Illumina, San Diego, CA) following the manufacturer's protocols. One lane per sample was used for sequencing with the Illumina Genome Analyzer IIx (Illumina) to generate nondirectional, single-ended, 36-base pair reads. Quality-filtered reads were mapped to the reference genome sequences (NCBI Bio-Project accession number PRJNA57623, identification number 57623) using CLRNASeq version 0.80 (Chunlab, Seoul, Korea). Relative transcript abundance was computed by counting the RPKM (78).

ROS measurement

Chemical hydrolysis of 2′,7′-dichlorofluorescin diacetate was performed following procedures described elsewhere (79). Briefly, 0.5 ml of 5 mM 2′,7′-dichlorofluorescin diacetate, dissolved in 100% ethanol, was reacted with 2 ml of 0.1 N NaOH at room temperature for 30 min. The reaction was stopped by adding 7.5 ml of 100 mM PBS, giving a final DCF concentration of 50 μM. Bacterial suspensions prepared from stationary-phase

cultures were treated with 50 μg/ml tetracycline for 1 h. After treatment, the suspensions were centrifuged at 13,000 rpm for 3 min, and cell-free supernatants were removed. Cell pellets were resuspended with 50 μM DCF solution and incubated for 30 min. Then the DCF intensity, which is indicative of the intracellular ROS level, was measured with a Victor X4 plate reader (PerkinElmer Life Sciences).

SDS-PAGE analysis and protein identification

Preparation of periplasmic fractions followed procedures described previously (80). *V. cholerae* strains were grown anaerobically in LB for 16 h. Cell pellets were resuspended with PBS containing 250 μg/ml polymyxin B and incubated for 15 min at 4 °C. After incubation, the mixtures were centrifuged at 13,000 rpm for 20 min at 4 °C, and the supernatant was used for separation of periplasmic proteins. Protein was quantified by the method of Bradford, and 5 μg of proteins were separated by 12% SDS-PAGE. The SDS-polyacrylamide gel fractions were submitted to Yonsei Proteome Research Center for protein identification.

EPR analysis

Intracellular free iron levels were measured as described previously with a few modifications (47). Bacterial cells were grown in LB and harvested at 16 h post-inoculation. A bacterial cell pellet was resuspended in 5 ml of prewarmed fresh LB broth that contained 10 mM diethylentriaminepentaacetic acid, pH 7.0, and 20 mM desferrioxamine (pH 8.0). Diethylentriaminepentaacetic acid blocks further iron import, whereas desferrioxamine diffuses into cells and binds unincorporated iron in an EPR-visible ferric form. The concentrated cells were incubated at 37 °C for 15 min in a shaking incubator. The cells were washed with ice-cold 20 mM Tris-Cl (pH 7.4) twice. Cells were then resuspended in 200 μl of ice-cold 10% glycerol, 20 mM Tris-Cl (pH 7.4). The cell suspension (200 μl) then was transferred into an EPR tube and frozen in liquid nitrogen. Ferric sulfate standards were mixed with desferrioxamine and prepared in the same Tris buffer containing glycerol. The spectrometer settings were as follows: microwave power, 1 milliwatt; microwave frequency, 9.64 GHz; modulation amplitude, 10 Gauss at 100 KHz; temperature, 15 K.

Statistical analysis

The data are expressed as the means ± S.D. Unpaired Student's *t* tests (two-tailed, unequal variance) were used to analyze the differences between experimental groups. *p* values < 0.05 were considered statistically significant. All experiments were repeated for reproducibility.

Author contributions—H. Y. K., Y. T. O., and S. S. Y. conceptualization; H. Y. K. and Y. T. O. investigation; H. Y. K. and S. S. Y. writing-original draft; J. G. and K.-M. L. data curation; S. S. Y. supervision.

References

1. Faruque, S. M., Albert, M. J., and Mekalanos, J. J. (1998) Epidemiology, genetics, and ecology of toxigenic *Vibrio cholerae*. *Microbiol. Mol. Biol. Rev.* **62,** 1301–1314 Medline
2. Matson, J. S., Withey, J. H., and DiRita, V. J. (2007) Regulatory networks controlling *Vibrio cholerae* virulence gene expression. *Infect. Immun.* **75,** 5542–5549 CrossRef Medline
3. Thelin, K. H., and Taylor, R. K. (1996) Toxin-coregulated pilus, but not mannose-sensitive hemagglutinin, is required for colonization by *Vibrio cholerae* O1 El Tor biotype and O139 strains. *Infect. Immun.* **64,** 2853–2856 Medline
4. Childers, B. M., and Klose, K. E. (2007) Regulation of virulence in *Vibrio cholerae*: the ToxR regulon. *Future Microbiol.* **2,** 335–344 CrossRef Medline
5. Krebs, S. J., and Taylor, R. K. (2011) Protection and attachment of *Vibrio cholerae* mediated by the toxin-coregulated pilus in the infant mouse model. *J. Bacteriol.* **193,** 5260–5270 CrossRef Medline
6. Patra, F. C., Sack, D. A., Islam, A., Alam, A. N., and Mazumder, R. N. (1989) Oral rehydration formula containing alanine and glucose for treatment of diarrhoea: a controlled trial. *BMJ* **298,** 1353–1356 CrossRef Medline
7. Leibovici-Weissman Ya., Neuberger, A., Bitterman, R., Sinclair, D., Salam, M. A., and Paul, M. (2014) Antimicrobial drugs for treating cholera. *Cochrane Database Syst. Rev.* CD008625 CrossRef Medline
8. Greenough, W. B., 3rd, Rosenberg, I. S., Gordon, R. S., Jr., Davies, B. I., and Benenson, A. S. (1964) Tetracycline in the treatment of cholera. *Lancet* **1,** 355–357 Medline
9. Lindenbaum, J., Greenough, W. B., and Islam, M. R. (1967) Antibiotic therapy of cholera. *Bull. World Health Organ.* **36,** 871–883 Medline
10. Rahaman, M. M., Majid, M. A., Alam, A. K. M. J., and Islam, M. R. (1976) Effects of doxycycline in actively purging cholera patients: a double-blind clinical trial. *Antimicrob. Agents Chemother.* **10,** 610–612 CrossRef Medline
11. Roy, S. K., Islam, A., Ali, R., Islam, K. E., Khan, R. A., Ara, S. H., Saifuddin, N. M., and Fuchs, G. J. (1998) A randomized clinical trial to compare the efficacy of erythromycin, ampicillin and tetracycline for the treatment of cholera in children. *Trans. R. Soc. Trop. Med. Hyg.* **92,** 460–462 CrossRef Medline
12. Kaushik, J. S., Gupta, P., Faridi, M. M. A., and Das, S. (2010) Single dose azithromycin versus ciprofloxacin for cholera in children: a randomized controlled trial. *Indian Pediatr.* **47,** 309–315 Medline
13. De, S., Chaudhuri, A., Dutta, P., Dutta, D., De, S. P., and Pal, S. C. (1976) Doxycycline in the treatment of cholera. *Bull. World Health Organ.* **54,** 177–179 Medline
14. Weber, J. T., Mintz, E. D., Cañizares, R., Semiglia, A., Gomez, I., Sempértegui, R., Dávila, A., Greene, K. D., Puhr, N. D., and Cameron, D. N. (1994) Epidemic cholera in Ecuador: multidrug-resistance and transmission by water and seafood. *Epidemiol. Infect.* **112,** 1–11 CrossRef Medline
15. Towner, K. J., Pearson, N. J., Mhalu, F. S., and O'Grady, F. (1980) Resistance to antimicrobial agents of *Vibrio cholerae* El Tor strains isolated during the fourth cholera epidemic in the United Republic of Tanzania. *Bull. World Health Organ.* **58,** 747–751 Medline
16. Wang, R., Lou, J., Liu, J., Zhang, L., Li, J., and Kan, B. (2012) Antibiotic resistance of *Vibrio cholerae* O1 El Tor strains from the seventh pandemic in China, 1961–2010. *Int. J. Antimicrob. Agents* **40,** 361–364 CrossRef Medline
17. Jesudason, M. (2006) Change in serotype and appearance of tetracycline resistance in *V. cholerae* O1 in Vellore, South India. *Indian J. Med. Microbiol.* **24,** 152–153 CrossRef Medline
18. Chomvarin, C., Johura, F.-T., Mannan, S. B., Jumroenjit, W., Kanoktippornchai, B., Tangkanakul, W., Tantisuwichwong, N., Huttayananont, S., Watanabe, H., Hasan, N. A., Huq, A., Cravioto, A., Colwell, R. R., and Alam, M. (2013) Drug response and genetic properties of *Vibrio cholerae* associated with endemic cholera in north-eastern Thailand, 2003–2011. *J. Med. Microbiol.* **62,** 599–609 CrossRef Medline
19. Mandal, J., Dinoop, K. P., and Parija, S. C. (2012) Increasing antimicrobial resistance of *Vibrio cholerae* OI biotype EI Tor strains isolated in a tertiary-care centre in India. *J. Health Popul. Nutr.* **30,** 12–16 Medline
20. Klontz, E. H., Das, S. K., Ahmed, D., Ahmed, S., Chisti, M. J., Malek, M. A., Faruque, A. S., and Klontz, K. C. (2014) Long-term comparison of antibiotic resistance in *Vibrio cholerae* O1 and *Shigella* species between urban and rural Bangladesh. *Clin. Infect. Dis.* **58,** e133–e136 CrossRef Medline

21. Oh, Y. T., Park, Y., Yoon, M. Y., Bari, W., Go, J., Min, K. B., Raskin, D. M., Lee, K.-M., and Yoon, S. S. (2014) Cholera toxin production during anaerobic trimethylamine *N*-oxide respiration is mediated by stringent response in *Vibrio cholerae*. *J. Biol. Chem.* **289,** 13232–13242 CrossRef Medline
22. Oh, Y. T., Lee, K.-M., Bari, W., Raskin, D. M., and Yoon, S. S. (2015) (p)ppGpp, a small nucleotide regulator, directs the metabolic fate of glucose in *Vibrio cholerae*. *J. Biol. Chem.* **290,** 13178–13190 CrossRef Medline
23. Magnusson, L. U., Farewell, A., and Nyström, T. (2005) ppGpp: a global regulator in *Escherichia coli*. *Trends Microbiol.* **13,** 236–242 Medline
24. Hauryliuk, V., Atkinson, G. C., Murakami, K. S., Tenson, T., and Gerdes, K. (2015) Recent functional insights into the role of (p)ppGpp in bacterial physiology. *Nat. Rev. Microbiol.* **13,** 298–309 CrossRef Medline
25. Potrykus, K., and Cashel, M. (2008) (p) ppGpp: still magical? *Annu. Rev. Microbiol.* **62,** 35–51 CrossRef Medline
26. Dalebroux, Z. D., and Swanson, M. S. (2012) ppGpp: magic beyond RNA polymerase. *Nat. Rev. Microbiol.* **10,** 203–212 CrossRef Medline
27. Gaca, A. O., Colomer-Winter, C., and Lemos, J. A. (2015) Many means to a common end: the intricacies of (p)ppGpp metabolism and its control of bacterial homeostasis. *J. Bacteriol.* **197,** 1146–1156 CrossRef Medline
28. Dalebroux, Z. D., Svensson, S. L., Gaynor, E. C., and Swanson, M. S. (2010) ppGpp conjures bacterial virulence. *Microbiol. Mol. Biol. Rev.* **74,** 171–199 CrossRef Medline
29. Das, B., Pal, R. R., Bag, S., and Bhadra, R. K. (2009) Stringent response in *Vibrio cholerae*: genetic analysis of *spoT* gene function and identification of a novel (p)ppGpp synthetase gene. *Mol. Microbiol.* **72,** 380–398 CrossRef Medline
30. Dasgupta, S., Basu, P., Pal, R. R., Bag, S., and Bhadra, R. K. (2014) Genetic and mutational characterization of the small alarmone synthetase gene *relV* of *Vibrio cholerae*. *Microbiology* **160,** 1855–1866 CrossRef Medline
31. Sikora, A. E. (2013) Proteins Secreted via the type II secretion system: smart strategies of *Vibrio cholerae* to maintain fitness in different ecological niches. *PLoS Pathog.* **9,** e1003126 CrossRef Medline
32. Aedo, S., and Tomasz, A. (2016) Role of the stringent stress response in the antibiotic resistance phenotype of methicillin-resistant *Staphylococcus aureus*. *Antimicrob. Agents Chemother.* **60,** 2311–2317 CrossRef Medline
33. Kim, C., Mwangi, M., Chung, M., Milheirço, C., de Lencastre, H., and Tomasz, A. (2013) The mechanism of heterogeneous β-lactam resistance in MRSA: key role of the stringent stress response. *PLoS One* **8,** e82814 CrossRef Medline
34. Abranches, J., Martinez, A. R., Kajfasz, J. K., Chávez, V., Garsin, D. A., and Lemos, J. A. (2009) The molecular alarmone (p)ppGpp mediates stress responses, vancomycin tolerance, and virulence in *Enterococcus faecalis*. *J. Bacteriol.* **191,** 2248–2256 CrossRef Medline
35. Wu, J., Long, Q., and Xie, J. (2010) (p)ppGpp and drug resistance. *J. Cell. Physiol.* **224,** 300–304 CrossRef Medline
36. Ishiguro, E. E., and Ramey, W. D. (1980) Inhibition of *in vitro* peptidoglycan biosynthesis in *Escherichia coli* by guanosine 5′-diphosphate 3′-diphosphate. *Can. J. Microbiol.* **26,** 1514–1518 CrossRef Medline
37. Rodionov, D. G., and Ishiguro, E. E. (1995) Direct correlation between overproduction of guanosine 3′,5′-bispyrophosphate (ppGpp) and penicillin tolerance in *Escherichia coli*. *J. Bacteriol.* **177,** 4224–4229 CrossRef Medline
38. Heath, R. J., Jackowski, S., and Rock, C. O. (1994) Guanosine tetraphosphate inhibition of fatty acid and phospholipid synthesis in *Escherichia coli* is relieved by overexpression of glycerol-3-phosphate acyltransferase (plsB). *J. Biol. Chem.* **269,** 26584–26590 Medline
39. Greenway, D. L. A., and England, R. R. (1999) The intrinsic resistance of *Escherichia coli* to various antimicrobial agents requires ppGpp and σs. *Lett. Appl. Microbiol.* **29,** 323–326 CrossRef Medline
40. Hesketh, A., Hill, C., Mokhtar, J., Novotna, G., Tran, N., Bibb, M., and Hong, H.-J. (2011) Genome-wide dynamics of a bacterial response to antibiotics that target the cell envelope. *BMC Genomics* **12,** 226 CrossRef Medline
41. Nguyen, D., Joshi-Datar, A., Lepine, F., Bauerle, E., Olakanmi, O., Beer, K., McKay, G., Siehnel, R., Schafhauser, J., Wang, Y., Britigan, B. E., and Singh, P. K. (2011) Active starvation responses mediate antibiotic tolerance in biofilms and nutrient-limited bacteria. *Science* **334,** 982–986 CrossRef Medline
42. Khakimova, M., Ahlgren, H. G., Harrison, J. J., English, A. M., and Nguyen, D. (2013) The stringent response controls catalases in *Pseudomonas aeruginosa* and is required for hydrogen peroxide and antibiotic tolerance. *J. Bacteriol.* **195,** 2011–2020 CrossRef Medline
43. Kohanski, M. A., Dwyer, D. J., Hayete, B., Lawrence, C. A., and Collins, J. J. (2007) A common mechanism of cellular death induced by bactericidal antibiotics. *Cell* **130,** 797–810 Medline
44. Lobritz, M. A., Belenky, P., Porter, C. B. M., Gutierrez, A., Yang, J. H., Schwarz, E. G., Dwyer, D. J., Khalil, A. S., and Collins, J. J. (2015) Antibiotic efficacy is linked to bacterial cellular respiration. *Proc. Natl. Acad. Sci. U.S.A.* **112,** 8173–8180 CrossRef Medline
45. Dwyer, D. J., Belenky, P. A., Yang, J. H., MacDonald, I. C., Martell, J. D., Takahashi, N., Chan, C. T. Y., Lobritz, M. A., Braff, D., Schwarz, E. G., Ye, J. D., Pati, M., Vercruysse, M., Ralifo, P. S., Allison, K. R., *et al.* (2014) Antibiotics induce redox-related physiological alterations as part of their lethality. *Proc. Natl. Acad. Sci. U.S.A.* **111,** E2100–E2109 CrossRef Medline
46. Pal, R. R., Bag, S., Dasgupta, S., Das, B., and Bhadra, R. K. (2012) Functional characterization of the stringent response regulatory gene *dksA* of *Vibrio cholerae* and its role in modulation of virulence phenotypes. *J. Bacteriol.* **194,** 5638–5648 CrossRef Medline
47. Jang, S., and Imlay, J. A. (2010) Hydrogen peroxide inactivates the *Escherichia coli* Isc iron-sulfur assembly system, and OxyR induces the Suf system to compensate. *Mol. Microbiol.* **78,** 1448–1467 CrossRef Medline
48. Ronayne, E. A., Wan, Y. C. S., Boudreau, B. A., Landick, R., and Cox, M. M. (2016) P1 Ref endonuclease: a molecular mechanism for phage-enhanced antibiotic lethality. *PLOS Genet.* **12,** e1005797 CrossRef Medline
49. Wang, X., Kim, Y., Ma, Q., Hong, S. H., Pokusaeva, K., Sturino, J. M., and Wood, T. K. (2010) Cryptic prophages help bacteria cope with adverse environments. *Nat. Commun.* **1,** 147 CrossRef Medline
50. Jubair, M., Morris, J. G., Jr., and Ali, A. (2012) Survival of *Vibrio cholerae* in nutrient-poor environments is associated with a novel "persister" phenotype. *PLoS One* **7,** e45187 CrossRef Medline
51. Imlay, J. A., Chin, S. M., and Linn, S. (1988) Toxic DNA damage by hydrogen peroxide through the Fenton reaction *in vivo* and *in vitro*. *Science* **240,** 640–642 CrossRef Medline
52. Jang, S., and Imlay, J. A. (2007) Micromolar intracellular hydrogen peroxide disrupts metabolism by damaging iron-sulfur enzymes. *J. Biol. Chem.* **282,** 929–937 CrossRef Medline
53. Yoon, M. Y., Min, K. B., Lee, K.-M., Yoon, Y., Kim, Y., Oh, Y. T., Lee, K., Chun, J., Kim, B.-Y., Yoon, S.-H., Lee, I., Kim, C. Y., and Yoon, S. S. (2016) A single gene of a commensal microbe affects host susceptibility to enteric infection. *Nat. Commun.* **7,** 11606 CrossRef Medline
54. Brandt, K. G., Castro Antunes, M. M., and Silva, G. A. (2015) Acute diarrhea: evidence-based management. *J. Pediatr.* **91,** S36–S43 CrossRef Medline
55. Das, J. K., Ali, A., Salam, R. A., and Bhutta, Z. A. (2013) Antibiotics for the treatment of cholera, shigella and cryptosporidium in children. *BMC Public Health* **13,** S10 CrossRef Medline
56. Leibovici-Weissman, Y., Neuberger, A., Bitterman, R., Sinclair, D., Salam, M. A., and Paul, M. (2014) Antimicrobial drugs for treating cholera. *Cochrane Database Syst. Rev.* CD008625 CrossRef Medline
57. Mwansa, J. C. L., Mwaba, J., Lukwesa, C., Bhuiyan, N. A., Ansaruzzaman, M., Ramamurthy, T., Alam, M., and Balakrish Nair, G. (2007) Multiply antibiotic-resistant *Vibrio cholerae* O1 biotype El Tor strains emerge during cholera outbreaks in Zambia. *Epidemiol. Infect.* **135,** 847–853 CrossRef Medline
58. Sugisaki, K., Hanawa, T., Yonezawa, H., Osaki, T., Fukutomi, T., Kawakami, H., Yamamoto, T., and Kamiya, S. (2013) Role of (p)ppGpp in biofilm formation and expression of filamentous structures in *Bordetella pertussis*. *Microbiology* **159,** 1379–1389 CrossRef Medline
59. Jiang, M., Sullivan, S. M., Wout, P. K., and Maddock, J. R. (2007) G-protein control of the ribosome-associated stress response protein SpoT. *J. Bacteriol.* **189,** 6140–6147 CrossRef Medline

60. Yoon, M. Y., Lee, K., and Yoon, S. S. (2014) Protective role of gut commensal microbes against intestinal infections. *J. Microbiol.* **52,** 983–989 CrossRef Medline
61. Potrykus, K., Murphy, H., Philippe, N., and Cashel, M. (2011) ppGpp is the major source of growth rate control in *E. coli*. *Environ. Microbiol.* **13,** 563–575 CrossRef Medline
62. Gaca, A. O., Kajfasz, J. K., Miller, J. H., Liu, K., Wang, J. D., Abranches, J., and Lemos, J. A. (2013) Basal levels of (p)ppGpp in *Enterococcus faecalis*: the magic beyond the stringent response. *mBio* **4,** e00646-13 Medline
63. Maisonneuve, E., Castro-Camargo, M., and Gerdes, K. (2013) (p)ppGpp controls bacterial persistence by stochastic induction of toxin-antitoxin activity. *Cell* **154,** 1140–1150 CrossRef Medline
64. Maisonneuve, E., and Gerdes, K. (2014) Molecular mechanisms underlying bacterial persisters. *Cell* **157,** 539–548 CrossRef Medline
65. Lewis, K. (2010) Persister cells. *Annu. Rev. Microbiol.* **64,** 357–372 CrossRef Medline
66. Wyckoff, E. E., Mey, A. R., Leimbach, A., Fisher, C. F., and Payne, S. M. (2006) Characterization of ferric and ferrous iron transport systems in *Vibrio cholerae*. *J. Bacteriol.* **188,** 6515–6523 CrossRef Medline
67. Griffiths, G. L., Sigel, S. P., Payne, S. M., and Neilands, J. B. (1984) Vibriobactin, a siderophore from *Vibrio cholerae*. *J. Biol. Chem.* **259,** 383–385 Medline
68. Mey, A. R., Wyckoff, E. E., Oglesby, A. G., Rab, E., Taylor, R. K., and Payne, S. M. (2002) Identification of the *Vibrio cholerae* enterobactin receptors VctA and IrgA: IrgA is not required for virulence. *Infect. Immun.* **70,** 3419–3426 CrossRef Medline
69. Wyckoff, E. E., Valle, A.-M., Smith, S. L., and Payne, S. M. (1999) A multifunctional ATP-binding cassette transporter system from *Vibrio cholerae* transports vibriobactin and enterobactin. *J. Bacteriol.* **181,** 7588–7596 Medline
70. Rogers, M. B., Sexton, J. A., DeCastro, G. J., and Calderwood, S. B. (2000) Identification of an operon required for ferrichrome iron utilization in *Vibrio cholerae*. *J. Bacteriol.* **182,** 2350–2353 CrossRef Medline
71. Davies, B. W., Bogard, R. W., and Mekalanos, J. J. (2011) Mapping the regulon of *Vibrio cholerae* ferric uptake regulator expands its known network of gene regulation. *Proc. Natl. Acad. Sci. U.S.A.* **108,** 12467–12472 CrossRef Medline
72. Brynildsen, M. P., and Liao, J. C. (2009) An integrated network approach identifies the isobutanol response network of *Escherichia coli*. *Mol. Syst. Biol.* **5,** 277 CrossRef Medline
73. Baharoglu, Z., and Mazel, D. (2011) *Vibrio cholerae* triggers SOS and mutagenesis in response to a wide range of antibiotics: a route towards multiresistance. *Antimicrob. Agents Chemother.* **55,** 2438–2441 CrossRef Medline
74. Wexselblatt, E., Oppenheimer-Shaanan, Y., Kaspy, I., London, N., Schueler-Furman, O., Yavin, E., Glaser, G., Katzhendler, J., and Ben-Yehuda, S. (2012) Relacin, a novel antibacterial agent targeting the stringent response. *PLoS Pathog.* **8,** e1002925 CrossRef Medline
75. Oh, Y. T., Kim, H. Y., Kim, E. J., Go, J., Hwang, W., Kim, H. R., Kim, D. W., and Yoon, S. S. (2016) Selective and efficient elimination of *Vibrio cholerae* with a chemical modulator that targets glucose metabolism. *Front. Cell. Infect. Microbiol.* **6,** 156 Medline
76. Philippe, N., Alcaraz, J.-P., Coursange, E., Geiselmann, J., and Schneider, D. (2004) Improvement of pCVD442, a suicide plasmid for gene allele exchange in bacteria. *Plasmid* **51,** 246–255 CrossRef Medline
77. Yoon, M. Y., Lee, K.-M., Park, Y., Yoon, S. S., and Kaushal, D. (2011) Contribution of cell elongation to the biofilm formation of *Pseudomonas aeruginosa* during anaerobic respiration. *PLoS One* **6,** e16105 CrossRef Medline
78. Fonseca, N. A., Marioni, J., and Brazma, A. (2014) RNA-Seq gene profiling: a systematic empirical comparison. *PLoS One* **9,** e107026 CrossRef Medline
79. Possel, H., Noack, H., Augustin, W., Keilhoff, G., and Wolf, G. (1997) 2,7-Dihydrodichlorofluorescein diacetate as a fluorescent marker for peroxynitrite formation. *FEBS Lett.* **416,** 175–178 CrossRef Medline
80. Lee, K.-M., Park, Y., Bari, W., Yoon, M. Y., Go, J., Kim, S. C., Lee, H-I., and Yoon, S. S. (2012) Activation of cholera toxin production by anaerobic respiration of trimethylamine *N*-oxide in *Vibrio cholerae*. *J. Biol. Chem.* **287,** 39742–39752 CrossRef Medline
81. World Health Organization (2014) Cholera, 2013. *Wkly. Epidemiol. Rec.* **89,** 345–355 Medline
82. World Health Organization (2012) Cholera, 2011. *Releve epidemiologique hebdomadaire* **87,** 289–304 Medline